

THIS IS THE ACCEPTED VERSION OF THE MANUSCRIPT

Please cite this article as: Groenewald, D.P., Day, M.O., Penn-Clarke, C.R., Rubidge, B.S. 2022, Stepping out across the Karoo retro-foreland basin: Improved constraints on the Ecca-Beaufort shoreline along the northern margin, *Journal of African Earth Sciences*, 185, 104389. doi: <https://doi.org/10.1016/j.jafrearsci.2021.104389>.

© 2022. This manuscript version is made available under the CC-BY-NC-ND 4.0 license <https://creativecommons.org/licenses/by-nc-nd/4.0/>

1 **STEPPING OUT ACROSS THE KAROO RETRO-FORELAND BASIN: IMPROVED**
2 **CONSTRAINTS ON THE ECCA-BEAUFORT SHORELINE ALONG THE**
3 **NORTHERN MARGIN.**

4 DAVID P. GROENEWALD, MICHAEL O. DAY, CAMERON R. PENN-CLARKE, AND
5 BRUCE S. RUBIDGE

6 The Karoo Supergroup of South Africa, internationally renowned for its almost continuous
7 Carboniferous to Jurassic record of deposition in a foreland basin setting, hosts an
8 unparalleled record of fossil tetrapods that provides unique insight into terrestrial biodiversity
9 change over this extended period. Understanding of the litho-, bio- and chronostratigraphy of
10 the Karoo Basin has greatly improved in recent years but most work has focused on the
11 thicker and better-exposed rocks in the basinal foredeep. A core issue that has remained
12 ambiguous is the stratigraphic placement of the diachronous Ecca-Beaufort contact, for which
13 different criteria have been used during mapping in different parts of the main Karoo Basin.
14 Comparison of biostratigraphy and contrasting lithological facies changes with those in the
15 better-studied foredeep enabled us to revise the lithostratigraphy of the Ecca and Beaufort
16 groups in the distal part of the main Karoo Basin. The presence of proximal marine facies
17 associations in the distal sector conform with the definition of the Waterford Formation of the
18 Ecca Group, so far recognised only in the southern foredeep. The upper contact of the
19 Waterford Formation represents a change from a subaqueous to a subaerial delta plain
20 depositional environment and marks the boundary between the Ecca and Beaufort groups, as
21 in the south. This has consequences for Beaufort Group stratigraphic subdivision in the distal
22 sector of the Karoo foreland basin.

23 **Keywords: Ecca Group, Beaufort Group, biostratigraphy, Permian, Ecca sea,**
24 ***Tapinocephalus* Assemblage Zone, *Daptocephalus* Assemblage Zone**

25 **Authors:**

26 *David P. Groenewald [david.groenewald@wits.ac.za], Evolutionary Studies Institute, School*
27 *of Geosciences, University of the Witwatersrand, Johannesburg, South Africa and Institut*
28 *Català de Paleontologia Miquel Crusafont, Edifici ICTA-ICP, c/ Columnes s/n, Campus de la*
29 *UAB, 08193 Cerdanyola del Vallès, Barcelona, Spain.*

30 *Michael O. Day [michael.day@nhm.ac.uk], Department of Earth Sciences, Natural History*
31 *Museum, London SW7 5BD, U.K. and Evolutionary Studies Institute, School of Geosciences,*
32 *University of the Witwatersrand, Johannesburg, South Africa.*

33 *Cameron R. Penn-Clarke [cpennclarke@geoscience.org.za], Council for Geoscience, 3 Oos*
34 *Street, Bellville, Cape Town 7535, South Africa and Evolutionary Studies Institute, University*
35 *of the Witwatersrand, Johannesburg, South Africa.*

36 *Bruce S. Rubidge [bruce.rubidge@wits.ac.za], Evolutionary Studies Institute, School of*
37 *Geosciences, University of the Witwatersrand, Johannesburg, South Africa.*

38 1 Introduction

39 The main Karoo Basin of South Africa, because of its wealth of fossils, excellent outcrops,
40 and dateable ash beds, has become an archetype for understanding deposition in foreland-
41 type depobasins (e.g. Catuneanu, 2004; Catuneanu et al., 2005). Based on differing
42 lithological characteristics, including facies, age, provenance, transport direction and stratal
43 stacking patterns, the main Karoo Basin has been divided into three regions: the proximal
44 south-western (west of 24° E), south-eastern (east of 24° E) and the distal northern or north-
45 eastern region (SACS, 1980; Catuneanu et al., 1998; Johnson et al., 2006). Reflecting this,
46 different lithostratigraphic names have been used to delineate the stratigraphy in these
47 different parts of the basin (Figure 1; SACS, 1980; Johnson et al., 2006). Revision of this
48 subdivision around the basin by the South African Committee for Stratigraphy (SACS) is
49 ongoing e.g. the synonymisation of the now defunct Koonap Formation with the
50 Abrahamskraal Formation of the Beaufort Group (Cole et al., 2016) and the amalgamation of
51 the Normandien Formation with the Balfour Formation on the 2019 1:1 000 000 Geological
52 map of South Africa (Council for Geoscience, 2019; D. Cole personal communication 2018,
53 2019).

54 Despite the well-developed litho- and biostratigraphic schemes for the Karoo Supergroup, the
55 stratigraphic placement of the contact between the Permian Ecca and Beaufort groups
56 remains inconsistently defined (e.g. Johnson, 1987). Previous criteria for determining the
57 contact range from the first appearance of “reptilian fossil remains” (Schwarz, 1896; Rogers
58 et al., 1909), the first appearance of “purplish shale or mudstone” (e.g. Mountain, 1946;
59 Keyser and Smith, 1979), the “base of the first sandstone displaying an erosive contact”
60 (Loock and Grobler, 1988), and the “base of the first prominent sandstone overlying the
61 argillaceous Ecca Group” (Rogers et al., 1909; Ryan, 1967; Zawada, 1988a; Zawada and
62 Cadle, 1988; Groenewald, 1989; Muntingh, 1989, 1997). This has resulted in mismatch of the

63 placement of the Ecca-Beaufort contact between the geographically distant proximal
64 (southern) and distal (northern) sectors of the main Karoo Basin.

65 This issue is compounded because the distal northern region has received less research
66 attention than the proximal south-western and south-eastern parts of the basin, where
67 outcrops are better exposed, and the stratigraphic sequence is most complete. Furthermore,
68 previous work on Permian Beaufort Group strata in the north of the basin (e.g. Theron, 1970;
69 Csaky and Wachsmuth, 1971; Cadle and Proedrou, 1975; Bars and Guillebert, 1976; Turner,
70 1977; Groenewald, 1984; Zawada, 1988a; Groenewald, 1989; Muntingh, 1997; Cole and
71 Wipplinger, 2001; Neveling, 2004; Rutherford, 2009; Mavuso, 2014; Rutherford et al., 2015)
72 had a strong focus on the sedimentology of the rock units, with only limited palaeontological
73 and biostratigraphic work being undertaken (e.g. Groenewald, 1989, 1990; Welman et al.,
74 2001; Hancox et al., 2002; Latimer et al., 2002; Rubidge et al., 2015; Rutherford et al., 2015;
75 Groenewald et al., 2019). Because of this, current understanding of vertebrate distribution in
76 the main Karoo Basin and mid- to late Permian Beaufort Group biostratigraphy is based
77 mostly on results from the southern parts of the basin (e.g. Kitching, 1977; Keyser and Smith,
78 1979; Rubidge, 1995, 2005; Mason, 2007; Rubidge et al., 2013; Mason et al., 2015; Smith et
79 al., 2020).

80 This paper reports on the sedimentary characteristics documented across the Ecca-Beaufort
81 contact in the distal sector of the main Karoo Basin (*sensu* Catuneanu et al., 1998) and
82 assesses whether the same criteria used to define the Ecca-Beaufort contact in the proximal
83 sector of the main Karoo Basin can be applied to these outcrops. Based on the stratigraphic
84 and geographic distribution of tetrapod fossils, we refine the biostratigraphy of the lowermost
85 Beaufort Group in the north of the main Karoo Basin and discuss the presence of the
86 Waterford Formation in the north of the basin and the consequent implications for the status
87 of the Normandien Formation.

88 2 Geological and palaeontological setting

89 Fieldwork was undertaken along the mapped Eccca-Beaufort contact in the distal sector of the
90 main Karoo Basin, from Philippolis in the Free State to Estcourt in KwaZulu-Natal (Figure
91 1). Rock units that were focused on include the uppermost Eccca Group (Tierberg, Volksrust,
92 and Waterford formations) and lowermost Beaufort Group (Adelaide Subgroup and
93 Normandien Formation).

94 2.1 Eccca Group

95 The Eccca Group in the Free State and KwaZulu-Natal Province comprises the Prince Albert,
96 Whitehill, Tierberg, Pietermaritzburg, Vryheid, Volksrust, and Waterford formations (SACS,
97 1980). Of these, the Tierberg, Volksrust, and Waterford formations comprise the upper part
98 of the Eccca Group in the field study area (Linström, 1973; Zawada, 1988a; Groenewald,
99 1989; Muntingh, 1989, 1997; Welman et al., 2001). Except for the Vryheid Formation, rocks
100 of the Eccca Group, are predominantly argillaceous and have been interpreted as having been
101 deposited in marine-to-marginal marine (paralic) settings (Johnson, 1976; Van Vuuren and
102 Cole, 1979; Cairncross and Cadle, 1988a, 1988b; Tavener-Smith et al., 1988; Cadle et al.,
103 1993; Veevers et al., 1994; Cairncross, 2001; Viljoen, 2005; Johnson et al., 2006; Green and
104 Smith, 2012; Hancox and Götz, 2014). While it is generally accepted that the lower part of
105 the Eccca Group (Prince Albert Formation) was deposited under marine conditions, several
106 studies suggest that the upper parts of the Eccca Group were deposited under brackish-to-fresh
107 water conditions (Zawada, 1988b; Veevers et al., 1994; Muntingh, 1997), with the Waterford
108 Formation representing the progradation of delta front and delta plain sands, and shallow
109 marine-shelf sediments (Rust et al., 1991; Smith et al., 1993; Rubidge et al., 2000; Cole and
110 Wipplinger, 2001).

111 2.2 Beaufort Group

112 This study focuses on rocks of the Adelaide Subgroup, which comprises a succession of
113 mudstones and sandstones generally interpreted as having been deposited in various
114 terrestrial fluvial to lacustrine environments (Smith et al., 1993; Johnson et al., 2006; Paiva,
115 2015). In the south-western part of the basin, the Adelaide Subgroup comprises sandstones
116 and mudrocks of the Abrahamskraal and Teekloof formations (Figure 1), with the former
117 characterised by the presence of a number of cherty beds and less red mudstone relative to the
118 overlying Teekloof Formation (Keyser and Smith, 1979; SACS, 1980). In the south-eastern
119 areas, it comprises the Abrahamskraal, Middleton and Balfour formations (Johnson, 1976;
120 Day and Rubidge, 2014; Cole et al., 2016; Viglietti et al., 2017a, 2017b). In the southern and
121 central Free State Province, individual formations within the Adelaide Subgroup have not yet
122 been formally recognised and the Beaufort Group is mapped only at subgroup level on the
123 most recent 1:250 000 geological map sheets. Using both lithological and biostratigraphic
124 data, however, Groenewald *et al.* (2019) were able to distinguish between the Abrahamskraal
125 and Balfour Formation in the southern Free State. Further north and east, in the eastern Free
126 State and KwaZulu-Natal provinces, the only formation of the Adelaide Subgroup is the
127 Normandien Formation, which has been equated with the now informal Estcourt Formation
128 of Linström (1973) in KwaZulu-Natal (Johnson et al., 2006; Bordy and Prevec, 2008).
129 Groenewald (1984, 1989) recognised four mappable units in the Normandien Formation
130 (from bottom to top): the arenaceous Frankfort, Rooinek, and Schoondraai members, and
131 argillaceous Harrismith Member (Figure 1). Two unnamed argillaceous intervals, rich in
132 fossil leaf impressions, separate the Rooinek Member from the underlying Frankfort and
133 overlying Schoondraai members, but the two are difficult to distinguish from one another in
134 the field (Groenewald, 1984; Claassen, 2008). It has been proposed (Groenewald, 2015;
135 Rammutla, 2016) that the majority of the Frankfort Member of the Normandien Formation,

136 which represents deposition under prodelta and lower delta-plain conditions, should be
137 considered the lithostratigraphic equivalent of the Waterford Formation and should therefore
138 be included within the Ecca Group rather than the Beaufort Group

139 Rocks of Abrahamskraal Formation host fossils of the *Eodicynodon* and *Tapinocephalus*
140 assemblage zones (Day and Rubidge, 2020; Rubidge and Day, 2020). The overlying Teekloof
141 Formation has yielded fossils of the *Endothiodon*, *Tropidostoma*, *Cistecephalus*,
142 *Daptocephalus* assemblage zones. Fossils of the *Cistecephalus*, *Daptocephalus*, and
143 *Lystrosaurus declivis* assemblage zones have been recovered from rocks of the Balfour
144 Formation (Smith et al., 2020), which is correlated with the Normandien Formation based on
145 the occurrence of *Dicynodon lacerticeps* and *Daptocephalus leoniceps* (Groenewald, 1990;
146 Smith et al., 1993).

147 2.3 Ecca-Beaufort Contact

148 In the southern Karoo Basin, the currently accepted lithostratigraphic contact between the
149 Ecca and Beaufort groups is taken at the Waterford- (uppermost Ecca Group) Abrahamskraal
150 (lowermost Beaufort Group) contact (Cole *et al.* 2016; Rubidge *et al.* 2012). This reflects a
151 change in depositional environment from subaqueous conditions to subaerial fluvial
152 environments (Johnson, 1976; Rubidge et al., 2000, 2012; Welman et al., 2001; Mason et al.,
153 2015). However, the Waterford Formation is not mapped north of 30° 40' S (1:1M
154 Geological Map 2019, Council for Geoscience, Pretoria), with the contact of the Ecca and
155 Beaufort groups instead being shown at the contact between the shales of the Tierberg or
156 Volksrust formations and the more arenaceous strata of the Adelaide Subgroup (Linström,
157 1973, 1981; Groenewald, 1984, 1987; Zawada, 1987a, 1988a; Zawada and Cadle, 1988;
158 Muntingh, 1989; Schutte, 1993; Muntingh, 1997). Lithofacies very similar to those of the
159 Waterford Formation, and interpreted as having been deposited in a prograding deltaic
160 environment, have been recorded in the north of the basin (Linström, 1973; Turner, 1977;

161 Groenewald, 1984; Zawada, 1988a; Zawada and Cadle, 1988; Muntingh, 1997). The presence
162 of the Waterford Formation has not, however, been formally recognised.

163 Welman *et al.* (2001) were the first to consider the Waterford Formation to be present in the
164 southern Free State near Philippolis and placed the Ecca-Beaufort contact at the top of this
165 formation. Similarly, strata mapped as lowermost Beaufort Group in the central and north-
166 eastern Free State and KwaZulu-Natal provinces were later considered representative of the
167 Waterford Formation, based on lithological and genetic similarities (Mavuso, 2014;
168 Groenewald, 2015; Rammutla, 2016).

169 3 Materials and Methods

170 Lithostratigraphic investigations involved measuring 16 vertical sections of natural outcrops
171 with Jacob's staff and Abney level, supplemented with data from the literature, and by
172 logging two borehole cores stored at the Council for Geoscience National Core Library at
173 Donkerhoek, Pretoria (see Supplementary Table 1 for the GPS coordinates and Groenewald
174 2021 for the individual sections). Because this study focussed on the Ecca-Beaufort contact,
175 sections were started in the upper parts of the Volksrust or Tierberg formations where
176 possible and measured upwards as high up into the Beaufort Group as the exposures
177 permitted in the southern and central Free State and KwaZulu-Natal, and to within the
178 arenaceous Schoondraai Member of Groenewald (1984) in the north-eastern Free State.
179 Features such as lithology, colour, sedimentary structures, palaeocurrent directions, nodules,
180 fossils, and burrows were all noted. These 18 stratigraphic logs were used to compile six
181 composite sections (Figure 2) that are representative of the interval through the Ecca-
182 Beaufort contact in the study area. This study uses the lithofacies, facies association, and
183 architectural element classification schemes modified from Miall (1996, 2016), Colombera *et*
184 *al.* (2013), and Gani and Bhattacharya (2007). Lithofacies types (hereafter also referred to as
185 facies) from the study area (presented in Results: Table 1) are given facies codes which

186 include an upper-case letter denoting lithology (gravel (G), sandstones (S), siltstone and
187 mudstone fines (F) and carbonates (Ca)) followed by a lower-case letter for characteristic
188 features such as sedimentary structures (e.g. r = ripple cross-lamination, t = trough cross-
189 stratification). Where outcrops permitted, architectural element analysis was conducted to aid
190 with palaeoenvironmental interpretation. Based on the geometry of three-dimensional bodies,
191 and arrangement of facies within, 14 principal architectural elements as defined for fluvial
192 systems by Miall (1985, 1996, 2006, 2016), Platt and Keller (1992), and Colombera et al.
193 (2012, 2013), and for deltaic systems by Gani and Bhattacharya (2007) and Ahmed *et al.*
194 (2014) were recognised (presented in Results: Table 2). Considering that invertebrate trace
195 fossils are decidedly more useful as indicators of sedimentary environments than for
196 biostratigraphic purposes (Ekdale et al., 1984; Seilacher, 2007; Buatois and Mángano, 2011;
197 Knaust and Bromley, 2012), ichnofossils have been included in the facies association
198 descriptions where applicable. The co-occurrence of different lithofacies types, architectural
199 elements, and ichnofossils allowed for five facies associations to be recognised (presented in
200 Results: Table 3).

201 Palaeontological investigation resulted in the discovery of 65 vertebrate fossils that are
202 curated at the Evolutionary Studies Institute (ESI). Their stratigraphic positions were
203 recorded on sections and location documented using a handheld GPS device. Vertebrate
204 fossils were mechanically prepared using air scribes and were identified by the authors and
205 visiting palaeontologists (F. Abdala, K. Angielczyk & C. Kammerer personal
206 communication). The sample was augmented by an additional 342 records of specimens from
207 the Beaufort Fossil Vertebrate database (Nicolas, 2007; Nicolas and Rubidge, 2009; van der
208 Walt et al., 2010). This database is maintained by the ESI and includes fossils stored at the
209 National Museum, Bloemfontein; the Evolutionary Studies Institute, Johannesburg; the
210 Council for Geoscience, Pretoria; Iziko Museum, Cape Town; KwaZulu-Natal Museum,

211 Pietermaritzburg; and Ditsong Museum, Pretoria. Although more fossils have been recovered
212 from the study area, many of these were collected historically, have poor provenance data
213 attached to them, and/or are too fragmentary or unprepared to be identified. Fossil tetrapod
214 taxa recovered from the study area were compared with those reported from the better
215 sampled southern parts of the basin to determine which vertebrate biozones are present in the
216 north of the main Karoo Basin.

217 4 Results

218 4.1 Facies analysis

219 The six composite sections shown in Figure 2 highlight the lateral differences in thickness of
220 geological formations in the north of the main Karoo Basin. Characteristics of the 15
221 different lithofacies types, the 14 recognised architectural elements, and the five facies
222 associations are summarised in Tables 1, 2, and 3, respectively, and illustrated on figures 3-6.
223 Facies associations 1, 2, and 3 form a (generally gradational) coarsening- and thickening-
224 upward succession (Figure 4A). Facies associations 1, 2 and 3 are always overlain by facies
225 associations 4 and 5, which together form discrete fining-upward successions.

226 4.1.1 Facies Association 1 (Prodelta)

227 *Description:* Facies Association 1 (FA1) comprises a monotonous succession of moderate
228 grey to dark grey (Munsell colour: N3 to N5) mudrocks and includes lithofacies types Fl and
229 Fm. Facies Association 1 shows an upwards change from predominantly horizontally
230 laminated and massive mudstones lower down to ripple-laminated and lenticular-to-wavy
231 bedded facies higher up, along with an increase in the abundance and thickness of sandstone
232 beds. This facies association, which is found throughout the study area, always occurs at the
233 base of the stratigraphic section (Figure 2 and 4) and corresponds to the Tierberg and
234 Volksrust formations of the Ecca Group. The Volksrust and Tierberg formations are between

235 100 and 300 metres thick within the study area (Linström, 1981; Muntingh, 1989; Schutte,
236 1993).

237 This mudrock dominated succession corresponds broadly to the “Prodelta Fines” (PF)
238 architectural element described by Gani and Bhattacharya (2007) and Ahmed *et al.* (2014),
239 based on the fine grain size, thickness, and lateral extent. Occasional thin (< 5 cm thick)
240 lenticular- and wavy-bedded lighter-coloured (N6 to N8) silts and very fine sands
241 corresponding to Frontal Splay (FS) architectural elements (Gani and Bhattacharya, 2007;
242 Ahmed et al., 2014) are present. These become thicker and more abundant higher up, at the
243 transition from Facies Association 1 (FA1) to Facies Association 2 (FA2) or Facies
244 Association 3 (FA3).

245 Facies Association 1 is characterised by a low diversity and abundance of ichnofossils,
246 mostly *Thalassinoides* and *Planolites isp.* (Figure 5). Putative limulid trackways have also
247 been reported from the upper Tierberg Formation in the southern portion of the study area
248 (Anderson, 1975). Stratabound sideritic concretions (< 30 cm) and calcareous nodules (up to
249 3 m in diameter) were commonly observed. Unidentifiable fossilized fish scales and bones
250 are sometimes present, either within the mudrock or in sideritic nodules. The calcareous
251 nodules typically weather to brown, or sometimes white, and may preserve sedimentary
252 structures such as ripple cross-lamination. The round sideritic concretions are similar to those
253 described from the Mississippian shales at Wardie, Scotland by Bojanowski and Clarkson
254 (2012), and were likely formed during early diagenesis of the fine-grained, organic-rich
255 sediments as a result of precipitation of Fe-bearing authigenic minerals (including siderite
256 and pyrite) prior to significant compaction. Facies Association 1 displays almost no lateral
257 variation throughout the study area and grades vertically into the proximal prodelta (FA2) or
258 lower shoreface (FA3) facies associations, both of which have a much higher proportion of
259 sandstones.

260 *Interpretation:* FA1 is interpreted to represent the deposition of silts and clays, predominantly
261 from suspension, in the prodelta environment. This is based on the fine-grained nature,
262 continuous lateral extent, thickness of the facies association, and its basal position in a
263 generally upwards coarsening succession. This interpretation follows studies based on similar
264 muddy facies associations (e.g. Olariu and Bhattacharya, 2006; Fielding, 2010; Ahmed et al.,
265 2014; Jorissen et al., 2018), and is in agreement with previous interpretations from the study
266 area (e.g. Zawada, 1988a; Muntingh, 1990; Cairncross et al., 2005). Deposition is considered
267 to have occurred predominantly from suspension settling in deeper water (beneath wave
268 base), forming finely laminated to massive beds of mudstone. Some of the massive
269 mudstones (Facies Fm) may have been deposited more rapidly, by hypo- and hyperpycnal
270 flow processes (Bhattacharya and MacEachern, 2009). Ripple and wavy laminations, and the
271 deposition of coarser-grained sediments, resulted from occasional influxes of higher energy
272 conditions such as during storms or from floods. The upwards change from predominantly
273 horizontally laminated and massive mudstones lower down to ripple-laminated and
274 lenticular-to-wavy bedded facies towards the top of FA1 records the progradation of the delta
275 front, associated with decreasing water depth, increasing energy conditions, and more
276 proximal deposition.

277 FA1 is considered to have been deposited under brackish to marine conditions. This
278 interpretation is supported by the presence of the ichnogenera *Thalassinoides* and *Planolites*,
279 the limulid trackways [reported by Anderson (1975)], and the bivalve *Megadesmus*
280 (Cairncross et al., 2005). Marine to brackish conditions during deposition are further
281 supported by trace element analyses undertaken for the uppermost Tierberg and Volksrust
282 formations in the study area (Zawada, 1988b; Muntingh, 1997).

283 A depauperate ichnofauna may result from a stressed, including brackish, environment
284 (MacEachern et al., 2005; James and Dalrymple, 2010). It has also been noted that

285 bioturbation density and trace diversity tends to decrease in an offshore direction, e.g. the
286 sharp decrease in diversity and density of trace fossils below ~35 m water depth in the Gulf
287 of Mexico (Dashtgard et al., 2015). The general low abundance and diversity of ichnofossils
288 observed in FA1 suggest that the muds were deposited under dysaerobic conditions, or at
289 least in water with lower dissolved oxygen levels (MacEachern et al., 2005; Dashtgard et al.,
290 2015). Such conditions may be linked to poor circulation or turnover of the water column in
291 distal settings below wave-base (MacEachern et al., 2005).

292 4.1.2 Facies Association 2 (Delta front)

293 Facies Association 2 (FA2) includes the lithofacies types Fl, Fm, R, and Sd, with defined
294 sandstone sheets comprising Shx, Sa, Sr, Sh, and Sm. Architectural elements in this facies
295 association include Frontal Splays (FS) and Storm Sheets (SS; Figure 4; Table 2).

296 Architectural elements of FA4, including Sediment-Gravity-Flow Deposits (SG), Bar
297 Accretion (BA), and Channel Fill (CH) elements, are sometimes bounded by FA2 deposits.

298 Mudstones of FA2 are commonly dark to medium grey (N3 - N5) and sometimes yellow to
299 pale olive (5Y6/4 to 10Y 6/2) in colour. Siltstones and sandstones are typically lighter in
300 colour, generally varying between medium light grey to light grey (N6 – N8), and
301 occasionally light brown (5YR 6/4). Between the towns Kroonstad and Newcastle, rocks of
302 this facies association, and lithofacies type R in particular, are mica rich.

303 Plant remains comprising fossil wood pieces and fragmentary, and occasionally more
304 complete, *Glossopteris* leaf and horsetail stem impressions are common (see Groenewald,
305 2021 for examples). Occasional fish scales and bones are present in the mudstones or in
306 sideritic nodules. The density of bioturbation structures and number of identifiable
307 ichnogenera is similar to that observed in FA3 and is much greater than in the other facies
308 associations. The bioturbation index (BI; MacEachern et al., 2010) is normally between 1 and

309 3 but may be as high as 4 locally. Ichnogenera observed in FA2 include *Arenicolites*,
310 *Cochlichmus*, *Diplocraterion*, *Lockeia*, *Gyrochorte*, *Gordia*, *Ophiomorpha*, *Palaeophycus*,
311 *Planolites*, *Rosselia*, *Rusophycus*, *Skolithos*, *Teichichnus*, and *Thalassinoides* (Figure 5).

312 Ground up plant material, similar to the “coffee grounds” reported from the Mississippi delta
313 (Tye and Kisters, 1986) and the Waterford Formation in the southern portion of the basin
314 (Rubidge, 1988; Rubidge et al., 2000), is relatively common in siltstone or sandstone beds of
315 Facies R. Sandstone beds generally become thicker towards the top of FA2. In the study area,
316 FA2 overlies FA1 with a gradational contact. Facies association 2 may grade upwards into
317 FA3, or have a sharp, sometimes truncated contact with FA3 or FA4 (Figure 4). Laterally,
318 FA2 may interfinger with either FA1 or FA3.

319 *Interpretation:* FA2 is interpreted as being deposited on the delta front and in
320 interdistributary areas and bays. This interpretation is supported by its stratigraphic position,
321 the predominance of shallow-marine indicating horizontal traces (Buatois and Mángano,
322 2011), the presence of asymmetrical and symmetrical ripples, indicating both fluvial and
323 wave influence, and hummocky cross-stratification suggesting periodic storm influence
324 (Dumas and Arnott, 2006). Under normal conditions, the CH and BA elements of FA4, which
325 are present at the top of the overall upward coarsening succession, are interpreted to have
326 accumulated in the more proximal areas of the delta front with finer material being deposited
327 more distally. Periods of higher discharge, e.g. during flooding, and by migration and
328 reworking of sediment from distributary mouth bars and splay elements by longshore
329 currents, waves, and periodic storms (Elliott, 1974; Coleman and Prior, 1982; Walker and
330 James, 1992; Bhattacharya, 2010), could have resulted in coarser material being introduced to
331 the prodelta. Reworking of this coarser material by waves and during storms produced the SS
332 elements. Lithofacies type R indicates alternations between higher energy periods, during
333 which the coarser grained beds were deposited as FS elements, and periods of low-to-very

334 low energy, including during the waning period of a storm, during which the finer-grained
335 interbeds were deposited by suspension settling. Splay deposits were reworked by waves and
336 during storms, as evidenced by the abundance of wave and local hummocky cross-
337 stratification. Higher up in the section, thicker beds of lithofacies types Fm and Fl that
338 interfinger with lithofacies type R, and locally display extensive bioturbation, represent
339 deposition under quiet water conditions of the interdistributary bay. Here the coarser beds of
340 lithofacies type R were likely deposited as sheets following crevassing or overbank flooding
341 of the channels into the interdistributary bays, with levées being formed immediately adjacent
342 to the distributary channel (Elliott, 1974; Zawada, 1988a; Groenewald, 1989; Muntingh,
343 1997). Closer to the distributary channels, this resulted in the formation of levée deposits. In
344 the eastern portion of the study area, FS elements that display an alternation of sedimentary
345 structures within the same bed e.g. horizontally-laminated to massive to ripple-laminated,
346 have previously been interpreted as turbidite deposits with incomplete Bouma sequences
347 (Muntingh, 1997; Selover and Gastaldo, 2005). However, hyperpycnal flow deposits on the
348 delta front have been noted to resemble turbidite deposits from deep-water settings, and often
349 display a similar alternation of sedimentary structures linked to the pulsatory nature of the
350 flow (Mulder et al., 2003; Olariu et al., 2005, 2010). Such flows are common in fluvial-
351 dominated deltaic environments, and are triggered by flood events of the feeder river, with
352 thicker (0.5 m to 1 m thick) beds of horizontally laminated sandstones (within element FS)
353 being attributed to sustained hyperpycnal flows (Plink-Björklund and Steel, 2004; Petter and
354 Steel, 2006; Olariu et al., 2010). Higher discharge rates of the feeder river, and a
355 correspondingly high rate of sedimentation on the delta front, resulted in subaqueous density
356 flows (element SG of FA4) and abundant soft sediment deformation features (lithofacies type
357 Sd; (Coleman and Prior, 1978; Shanmugam, 2006; Bhattacharya, 2010).

358 4.1.3 Facies Association 3 (Lower shoreface)

359 The sandstone-dominated Facies Association 3 (FA3) is characterised by a predominance of
360 non-amalgamated to amalgamated cosets of lithofacies type Shx, with subordinate bedsets of
361 lithofacies type R, and minor, often bioturbated, interbedded mudstones of lithofacies type
362 Fm and Fl (Figure 4). Architectural element SS, comprising single or stacked beds of Shx, is
363 the main element present within this facies association. FA3 is poorly expressed in the field
364 study area and is best exposed at the Barend Wessel Dam at the town of Kroonstad (Figure
365 4). Here FA3 gradationally overlies FA1 and is sharply overlain by sandstones of FA4.
366 Abundant fragmentary plant material, similar to the “coffee grounds” reported from the
367 Mississippi delta (Tye and Kusters, 1986), are present in some of the sandstone beds. The
368 bioturbation index of FA3 ranges from 1- 3. FA3 hosts a similar diversity of ichnogenera to
369 that of FA2, with *Arenicolites*, *Cruziana*, *Gyrochorte*, *Ophiomorpha*, *Palaeophycus*,
370 *Planolites*, *Rosselia*, *Skolithos*, and *Thalassinoides* being identified during this study (Figure
371 5).

372 *Interpretation:* FA3 is interpreted as being deposited on the lower shoreface in a wave- and
373 storm-dominated shallow marine environment. Such environments are typically situated at or
374 above storm-wave base and are subject to periodic stormweather conditions, during which
375 time storm sheet deposits are formed under storm-related oscillatory and unidirectional
376 current hydrodynamic conditions, as well as suspension sedimentation conditions during fair
377 weather conditions (Bhattacharya and Giosan, 2003; Bhattacharya, 2010; Plint, 2010; Penn-
378 Clarke et al., 2019). Ichnofossils from FA3 are typical of the *Cruziana* ichnofacies, which is
379 generally interpreted to occur in shallow marine environments on the lower shoreface to
380 lower offshore zone (Seilacher, 2007; Buatois and Mángano, 2011).

381 4.1.4 Facies Association 4 (Confined Channelised deposits)

382 Facies Association 4 (FA4) comprises upward-fining, single- to multi-storey sandstones up to
383 30 m thick. Lithofacies types present in FA4 include Ss, St, Sh, Sp, Sr, Sm, Sa, and Sd, with
384 occasional occurrences of Gmm. Architectural elements identified from this facies
385 association include Channel Fill (CH), Bar Accretion (BA), Sediment-Gravity-Flow Deposits
386 (SG), Sandy Bedforms (SB), Lateral Accretion (LA) macroforms, Downstream Accretion
387 (DA) macroforms, and Downstream and Lateral Accretion (DLA) macroforms (Table 2;
388 Figure 4 and 6). When present, elements BA and CH are usually found in close association
389 and are best developed towards the top of the overall upwards-coarsening succession from
390 FA1 to FA2 or FA3 (i.e. the Waterford Formation). Elements CH, DA, and LA are typically
391 found in close association and are generally bounded by, or associated with, elements of FA5.
392 Bioturbation is uncommon and, where present, is generally restricted to the upper surfaces of
393 rippled sandstone beds.

394 Sandstone colours vary from light to very light grey (N7 – N8), light olive grey (5Y 6/1),
395 yellowish grey (5Y 7/2), greenish grey (5GY 6/1) yellow to pale olive (5Y 6/4 to 10Y 6/2),
396 and pale greenish yellow (10Y 8/2), often weathering to a more yellowish orange colour
397 (10YR 8/6 or 10YR 6/6). Carbonate concretions 0.3 m to > 2 m in diameter are present in
398 sandstone bodies of FA4 throughout the study area but are more abundant in sandstones from
399 the interval straddling the Ecca-Beaufort contact. A diagenetic origin for these concretions is
400 likely, based on their round shape and the fact that they often preserve sedimentary structures
401 not seen in the surrounding rock (Marshall and Pirrie, 2013). FA4 is relatively conspicuous in
402 the study area because of the cliff-forming nature of the sandstone deposits.

403 *Interpretation:* FA4 is interpreted to represent deposition by predominantly fluvial processes
404 on the proximal delta front to alluvial plain. Where CH and BA elements are found in
405 intimate association, typically overlying or interbedded with FA2 deposits, these elements are

406 interpreted to represent distributary channels (CH) and proximal mouth bars (BA) deposits on
407 the proximal delta front to lower delta plain environment. Some of the channelised elements
408 contain abundant floating clasts (Facies Sa) and may show stratification. These are similar to
409 channel deposits described from the Wall Creek Member of the Cretaceous Raptor Delta
410 (Gani and Bhattacharya, 2007) and from the Jackfork Group (Shanmugam, 2006) and are
411 interpreted to be sediment density flow deposits (element SG) that likely formed during
412 periods of higher discharge. Bar elements, formed through the migration of dunes within the
413 distributary channels, and mouth-bar deposits, which form at the mouths of channels due to
414 the change in flow conditions from confined to unconfined flow, and the associated sharp
415 decrease in velocity (Wright, 1977; Olariu and Bhattacharya, 2006), coalesce to form bar
416 assemblages that are intimately associated with the distributary channels. The generally low
417 intensity of bioturbation present in these deposits (BI 0 – 1) suggests proximity to the river
418 mouth (MacEachern et al., 2005; Gani and Bhattacharya, 2007). Delta lobe switching and
419 abandonment or a decrease in sediment supply from the feeder river, followed by wave
420 reworking and winnowing of the finer-grained sediments, may have resulted in the
421 development of cheniers along the coastline (Augustinus, 1989; Muntingh, 1997; Gani and
422 Bhattacharya, 2007; Bhattacharya, 2010; Plint, 2010).

423 In most localities in the study area, the distributary channels and bar complexes are, in turn,
424 overlain by fluvial channel deposits (often with erosive bases and pebble lags concentrated at
425 the base) and their associated overbank deposits (FA5). These deposits, characterised by
426 architectural elements CH, SB, DA, LA, and DLA, often occur in intimate association with
427 elements of FA5 and are interpreted to be deposited on the subaerial upper delta and alluvial
428 plain. However, at some localities e.g. Kalkwal and Brandfort hill (locality 3: Figure 2),
429 erosive based channels with pebble lags at the base directly overly FA2 deposits and the
430 distributary channels, bar complexes, and upper part of the genetically related prodelta

431 deposits are considered to have been eroded away (Loock and Grobler, 1988). The
432 characteristics of this suggests either a shallow platform (Galloway, 1975) or potentially a
433 period of forced regression (Bhattacharya, 2010; Plint, 2010).

434 4.1.5 Facies Association 5 (Floodplain fines and overbank deposits)

435 Facies Association 5 (FA5) always occurs in intimate association with FA4 and is the most
436 common facies association in the Abrahamskraal and Balfour formations in the study area.
437 This mudrock dominated facies association comprises lithofacies types Fl, Fm, C, Ca, Ss, Sr,
438 Sd, Sh, and Sm, and four principal architectural elements have been recognised, including
439 Overbank (floodplain) Fines (FF), Abandoned Channel (AC), Crevasse Splay (CS), and
440 Levées (LV; Table 2; Figure 6). Abundant slickensides, desiccation cracks, silicified gypsum
441 roses, blocky and fissile weathering features, articulated and disarticulated vertebrate fossils,
442 large and small fragments of silicified wood, plant rootlets, and extensive nodular horizons
443 (Figure 6) are all features that commonly occur within FA5 deposits and provide evidence for
444 subaerial exposure and palaeosol development (Smith, 1990; Retallack, 2001; Miall, 2006;
445 Smith and Botha-Brink, 2014). Because the finer grained facies tend to weather rapidly and
446 are often covered with scree and/or vegetation, outcrops of FA5 within the study area are
447 largely restricted to erosional dongas, steep unvegetated slopes, or man-made cuttings. This
448 makes the description of vertically and laterally continuous sequences difficult.

449 Mudstone colours of FA5 vary depending on the stratigraphic and geographic position. In the
450 southern Free State Province, the mudrocks of the Abrahamskraal Formation are
451 predominantly greenish grey (5G 6/1), moderate yellow green (5G 5/2), and greenish grey
452 (5GY 6/1). This is quite different to what is observed in the overlying Balfour Formation,
453 where mudrock colours include blackish red (5R 2/2), brownish grey (5YR 4/1), greyish red
454 (5R 4/2), greenish grey (5G 6/1 and 5GY 6/1), yellowish grey (5Y 7/2), pale olive (10Y 6/2),
455 and dusky yellow green (5GY 5/2). In the central Free State Province, mudrocks are

456 predominantly dusky yellow green (5GY 5/2), greenish grey (5GY 6/1) and pale olive (10Y
457 6/2), with brownish grey (5YR 4/1) and greyish red (5R 4/2) mudrocks only observed at the
458 locality Esbachskop near the town of Brandfort. In the north-eastern Free State and KwaZulu-
459 Natal provinces, mudrocks of FA5 are greyish olive (10Y 4/2), light olive grey (5Y 5/2), pale
460 olive (10Y 6/2), dusky yellow (5Y 6/4), dark greenish grey (5G 4/1), olive grey (5Y 3/2),
461 dark greenish yellow (10Y 6/6), moderate yellow (5Y 7/6), light olive brown (5Y 5/6),
462 medium grey (N5), and light blueish grey (5B 7/1).

463 *Interpretation:* FA5 is interpreted as terrestrial floodplain deposits, predominantly from
464 suspension settling (FF), with intermittent higher energy splay (CS) and levée (LV) deposits.
465 Floodplains typically act as sinks for finer material in alluvial systems, and are predominantly
466 formed by vertical accretion during floods, with lateral accretion deposits being of minor
467 importance (Nanson and Croke, 1992; Wright and Marriott, 1993). Deposition occurred in
468 temporary bodies and pools of standing water following flood events, or in semi-permanent
469 to permanent shallow lakes on the flood plain that allowed for the development of palustrine
470 carbonates (Ca). The presence of thin coal beds (C) and highly carbonaceous shales
471 interbedded within the FA5 deposits provides evidence for the existence of marshes in the
472 interdistributary areas and in low-lying areas of the alluvial floodplain (Miall, 2006, 2016).
473 Where floodplain accumulation was slow enough, and occurred over long periods, soil
474 formation processes began. This is evidenced by the abundant presence of palaeosol horizons
475 rich in carbonate nodules, colour mottling, plant rootlets and slickensides (Retallack, 1990;
476 Smith, 1990). The presence of mud crack features indicate that the alluvial floodplain was
477 subject to periodic drying.

478 4.2 Palaeontology

479 A total of 407 identifiable tetrapod fossils have been recovered from the study area. These
480 include a variety of dicynodont anomodonts, cynodonts, gorgonopsians, therocephalians, a

481 biarmosuchian, rhinesuchid amphibians, and the reptile *Eunotosaurus africanus* (Table 4).
482 Stratigraphic ranges of vertebrate fossils collected during this study are indicated on the
483 composite stratigraphic logs (Figure 2). For the full list of tetrapod fossils used for this study,
484 please see Supplementary Table 2 and Groenewald (2021) for photographs and
485 identifications.

486 Two distinctive and stratigraphically disparate faunal assemblages were recovered in the
487 Beaufort Group of the southern Free State (Figure 2; Groenewald et al., 2019; Groenewald,
488 2021). The lower of these is characterised by an abundance of *Eosimops* specimens in
489 association with *Robertia*, *Pristerodon*, *Eunotosaurus*, and the scylacosaurid therocephalian
490 *Glanosuchus* and is assigned to the middle Permian (Capitanian) *Glanosuchus-Eosimops*
491 *subzone* of the *Tapinocephalus* AZ (Groenewald et al., 2019; Day and Rubidge, 2020). The
492 upper assemblage, characterised by an abundance of *Oudenodon* specimens in association
493 with *Rhachiocephalus*, *Aulacephalodon*, *Diictodon*; *Basilodon*; *Dinanomodon*, and
494 gorgonopsians, is assigned to the late Permian (Lopingian) uppermost *Cistecephalus* AZ or
495 the *Dicynodon-Theriognathus* subzone of the *Daptocephalus* AZ (Groenewald et al., 2019;
496 Smith, 2020; Viglietti, 2020; Groenewald, 2021).

497 Northwards, around Bloemfontein, the stratigraphically lowest tetrapod fossils recorded in
498 the Beaufort Fossil Vertebrate database were collected from the locality Kranskraal. This
499 locality is situated approximately 22 km northeast of Bloemfontein along exposures adjacent
500 to the Modder River and has yielded the holotypes of *Rhachiocephalus angusticeps* (Broom,
501 1937) and *Compsodon helmoedi* (van Hoepen, 1934) along with specimens of *Oudenodon*
502 *bainii* and the gorgonopsid *Arctognathus curvimola*, all of which have stratigraphic ranges
503 extending from the *Cistecephalus* to lower *Daptocephalus* AZs. The specimen number and
504 whereabouts of the holotype of *Rhachiocephalus angusticeps* is not known but the species is
505 considered synonymous with *Rhachiocephalus magnus*, as listed in Kitching (1977).

506 The Beaufort Fossil Vertebrate database records numerous fossils that have been recovered
507 from up to 100 m (based on elevation) stratigraphically higher than the fossils from
508 Kranskraal. The recovered taxa include *Oudenodon bainii*, *Daptocephalus/Dicynodon*, and
509 *Theriongnathus microps*. East of this, in the Thaba ‘Nchu district, *Lystrosaurus* is the most
510 abundant genus collected, with over 90 specimens representing the species *L. maccaigi*, *L.*
511 *murayi*, *L. curvatus*, *L. declivus*. Other genera from this area include *Daptocephalus*
512 *leoniceps*, *Dicynodon lacerticeps*, *Oudenodon bainii*, *Moschorhinus kitchingi*, *Scaloposaurus*
513 *constrictus*, *Vetusodon elikhulu* and *Procolophon trigoniceps*.

514 Farther north, between Brandfort and Kroonstad, exposures of the lowermost Beaufort Group
515 become sparser and the tetrapod species recovered closest to the Ecca-Beaufort contact in this
516 part of the basin are limited to an undescribed burnetiid specimen (BP/1/8262), the only
517 specimen of the therocephalian *Zorillodontops gracilis* (SAM-PK-K1392), and some
518 rhinesuchid temnospondyl material, including an axial skeleton from the Farm Malana
519 (BP/1/8195) that is tentatively identified as *Uranocentrodon senekalensis* (Groenewald,
520 2021). East of this, in the area between the towns Excelsior and Verkeerdevlei,
521 *Theriongnathus microps* co-occurs with *Oudenodon bainii* and *Aulacephalodon bainii*.

522 Rocks of the Balfour Formation (Normandien Formation) in the eastern Free State have
523 yielded a diverse faunal assemblage [Figure 2; (Groenewald, 2021)] that includes
524 *Daptocephalus leoniceps*, *Dicynodon lacerticeps*, *Dinanomodon gilli*, *Oudenodon bainii*,
525 *Kitchinganomodon crassus*, *Rhachiocephalus magnus*, *Lystrosaurus spp.*, rhinesuchids (e.g.
526 *Laccosaurus*), gorgonopsians, and an unidentified cynodont. Here some stratigraphic
527 separation of taxa is evident, with the large dicynodonts *Rhachiocephalus magnus* and
528 *Kitchinganomodon crassus* both restricted to the stratigraphic interval from immediately
529 below to just above the arenaceous Rooinek Member, and the stratigraphically lowest large

530 *Lystrosaurus* specimens (based on catalogue information) recovered from the argillaceous
531 interval immediately underlying the Schoondraai Member (Figure 2).

532 Fossils recovered from the Estcourt district of KwaZulu-Natal include *Daptocephalus*
533 *leoniceps*, *Dicynodon lacerticeps*, and *Oudenodon bainii*, and a rhinesuchid amphibian (c.f.
534 *Laccosaurus*). Further south, at Oatesdale Quarry near Mooi River, three specimens
535 identified as *Lystrosaurus maccaigi* were found in close association with a *Dicynodontoides*
536 mandible, the partial axial skeleton of an unidentified cynodont, and an isolated gorgonopsian
537 canine. The quarry is situated roughly 50 m below the sandstones of the Katberg Formation
538 and these specimens are therefore from the upper Balfour Formation (Viglietti et al., 2017b,
539 2021).

540 5 Discussion

541 5.1 Lithostratigraphy

542 The overall coarsening- and thickening-upward succession formed by Facies associations 1, 2
543 and/or 3, and 4 in the study area is typical of a prograding delta front or shoreface (Moore,
544 1966; Collinson and Thompson, 1989; Walker and James, 1992; James and Dalrymple,
545 2010), whereas the overlying FA5 (and in places FA4 when found in association with FA5),
546 which form discrete upward fining successions, are more typical of alluvial (fluvial and
547 floodplain) deposits (Walker and James, 1992; Miall, 2006, 2016; James and Dalrymple,
548 2010). We therefore interpret the studied stratigraphic interval as recording an upwards
549 change from deposition on the prodelta, through the delta front or lower shoreface, on the
550 lower delta plain, and finally on the upper delta plain. This is in broad agreement with
551 interpretations of previous workers (Linström, 1973; Botha and Linström, 1977; Turner,
552 1977; van Dijk et al., 1978; Zawada, 1988a; Groenewald, 1989; Muntingh, 1997; Welman et
553 al., 2001).

554 In this study, we consider rocks of FA1 to belong to the Tierberg or Volksrust formations of
555 the Ecca Group. Where FA4 and FA5 are found in association, we consider the rocks to
556 belong to the Beaufort Group. The intermediate stratigraphic interval, which separates the
557 mudrocks of the Tierberg/Volksrust formations (Ecca Group; FA1) from those of the
558 overlying fluviially dominated Beaufort Group (FA4 and FA5), contains a unique association
559 of lithofacies types and facies associations (FA2, FA3, and FA4) that can be recognised both
560 in the field and in borehole core. In the north-eastern part of the basin, this interval, which
561 broadly corresponds with Groenewald's (1984, 1989) Frankfort Member of the Normandien
562 Formation, has previously been included within the Beaufort Group. Elsewhere in the study
563 area, this interval includes rocks previously assigned to both the uppermost Ecca and
564 lowermost Beaufort groups. The interval is 30-45 m thick in the southern and north-eastern
565 Free State and thickens south-eastwards to more than 144 m near the town of Estcourt in
566 KwaZulu-Natal.

567 The rocks in this interval are here interpreted as having been deposited in a shallow marine
568 environment typified by both shoreface and deltaic environments. Deposition in a shallow
569 marine environment is supported by the ichnofaunal assemblages e.g. *Cruziana* ichnofacies,
570 while rhythmically interbedded sandstones/siltstones and mudstones (lithofacies type R)
571 indicate periodic (possibly seasonal) fluctuations in river discharge, with hyperpycnal flows
572 generating during flood events resulting in the deposition of frontal splay elements (element
573 FS). Evidence for high sedimentation rates include the abundance of soft-sediment
574 deformation structures (lithofacies type Sd) along with relatively abundant sediment gravity
575 and hyperpycnal flow deposits (elements FS and SG). Wave ripples and hummocky cross-
576 stratification (element SS) bear testament to periodic storm and wave influence on the
577 system. This interpretation is also in line with that of previous workers in the study area, who
578 all document several facies that are generally restricted to the interval between the Ecca and

579 Beaufort groups and interpret them as having been deposited in an essentially deltaic
580 environment (Linström, 1973, 1987; Turner, 1977; Botha and Linström, 1978; van Dijk et al.,
581 1978; Behounek, 1980; Zawada, 1987b, 1987a; Looock and Grobler, 1988; Groenewald, 1989,
582 2015; Muntingh, 1990, 1997; Green, 1997; Mavuso, 2014; Rammutla, 2016); although
583 Selover and Gastaldo (2005) suggested the presence of a deeper water turbidite system near
584 Estcourt.

585 Furthermore, some of the lithofacies that dominate this interval, and the interpreted
586 depositional environments, are very similar to those described from the Waterford Formation
587 of the Ecca Group by Rubidge et al. (2000) and Mason et al. (2015) from the south-western
588 and south-eastern main Karoo Basin, respectively. In particular, Rubidge's (1988) Facies A
589 and E, which are considered to be most diagnostic of the Waterford Formation further south
590 in the basin (Rubidge et al., 2000, 2012; Mason, 2007; Mason et al., 2015), correspond
591 directly with Lithofacies types R and Sd, respectively. Based on lithologic and genetic
592 similarities, we consider the stratigraphic interval where FA2, FA3, and FA4 occur to be
593 lithologically equivalent to the Waterford Formation, which forms the uppermost
594 stratigraphic unit of the Ecca Group in the south of the main Karoo Basin, and these rocks
595 should thus be included within the Ecca rather than the Beaufort Group. While younger in the
596 north than in the south (based on the biostratigraphy), we consider the Waterford Formation
597 to be present in the northern part of the main Karoo Basin. Here, it overlies the Tierberg or
598 Volksrust formations, forming the uppermost stratigraphic unit of the Ecca Group and
599 corroborating recent work (Welman et al., 2001; Mavuso, 2014; Groenewald, 2015;
600 Rammutla, 2016). The Waterford Formation is overlain by the Abrahamskraal Formation in
601 the southern Free State (Groenewald et al., 2019) and by the Balfour Formation in the central
602 and eastern Free State and KwaZulu-Natal.

603 For the purpose of mapping, the base of the first prominent sandstone was traditionally used
604 for the placement of the Eccca-Beaufort contact (Botha and Linström, 1978; Linström, 1981,
605 1987; Groenewald, 1984, 1987; Zawada, 1988a; Zawada and Cadle, 1988; Muntingh, 1989,
606 1997; Schutte, 1993). However, the current study has shown that this contact, as it outcrops
607 in the study area, corresponds to different stratigraphic horizons, e.g. it could represent either
608 the base of the Waterford Formation or a sandstone unit within it. As currently mapped, the
609 Waterford Formation in the study area encompasses strata assigned to the uppermost
610 Volksrust/Tierberg formations of the Eccca Group and/or the lowermost Adelaide
611 Subgroup/Normadien Formation of the Beaufort Group. Application of lithofacies analysis
612 can be used to map the different Facies Associations as discrete lithodemes, which can be
613 used to refine the lithostratigraphic placement of the contact between the Tierberg/Volksrust
614 and the Waterford formations, and between the Eccca and Beaufort groups. We suggest that
615 the top of both the Tierberg and Volksrust formations should be placed at the contact between
616 FA1 and FA2 or FA3. This is a similar contact to one that has previously been considered for
617 the Eccca-Beaufort contact in the southern Free State (Siebrits, 1987; Zawada and Cadle,
618 1988), and is the same as that proposed by Terblanche (1979) for the contact between the
619 Tierberg and Carnarvon [= Waterford (Cole and Wipplinger, 2001)] formations. To be
620 consistent with lithostratigraphic application in the rest of the basin, the Eccca-Beaufort
621 contact should be placed at the top of the Waterford Formation, at the point where FA4 and
622 FA5 predominate. This corresponds to the change from the lower to upper delta plain
623 environment and, at most localities, the contact can be placed at the base of a prominent
624 sandstone horizon with a basal pebble lag.

625 Groenewald *et al.* (2019) demonstrated that rocks of the lowermost Beaufort Group in the
626 southern Free State can be subdivided on both lithological and biostratigraphic grounds into a
627 lower and an upper interval, assignable to the Abrahamskraal and Balfour formations,

628 respectively. The most distinctive and easily observable lithological difference between the
629 two formations is the change in mudrock colours, with reddish mudstones [blackish red (5R
630 2/2), brownish grey (5YR 4/1) and greyish red (5R 4/2)] being almost entirely absent from
631 the Abrahamskraal Formation but predominant in the Balfour Formation.

632 While the data from this work is insufficient to positively attribute a fluvial style to the
633 Abrahamskraal Formation in the study area because of the paucity of good outcrop, a low
634 sinuosity fluvial style with ephemeral flow conditions as proposed by Zawada (1988a) is
635 supported by the abundance of SB and DA elements, coupled with high-consistency
636 palaeocurrent measurements (Groenewald, 2021), and the lack of features such as cut-banks
637 and major lateral accretion surfaces. Low sinuosity fluvial styles have also been identified
638 within the Abrahamskraal Formation in the south-western portion of the basin (Wilson et al.,
639 2014; Gulliford et al., 2014; Paiva, 2015). Finer material is interpreted as having been
640 deposited on the floodplain flanking the network of low-sinuosity streams. The presence of
641 lithofacies types F1 and Ca provide evidence for the development of floodplain lakes, while
642 the predominantly drab blueish colours of the mudrocks suggest a higher water table with
643 deposition under reducing conditions (Wilson et al., 2014; Bordy and Paiva, 2021).

644 Palaeocalcrete sheets similar to those described from the Teekloof Formation by Smith
645 (1990) are well exposed at Uitspankop (near locality 1: Figure 2) and possibly formed in the
646 zone of capillary rise just above the groundwater table. At several localities, including
647 Uitspankop, fossils were found as isolated skulls. This, coupled with the palaeocalcrete
648 sheets, is considered indicative of a proximal floodplain environment (Smith, 1990, 1993).

649 In the southern and central Free State, the Balfour Formation records a complex interaction
650 between a northern and southern fluvial system (Kingsley and Theron, 1964; Cole and
651 Wipplinger, 2001; Rutherford et al., 2015; Groenewald, 2021). Although the data from this
652 study do not allow a fluvial style to be positively attributed to the Balfour Formation in the

653 southern Free State, a high sinuosity fluvial style has been proposed based on the presence of
654 extensive lateral accretion surfaces (element LA) at Boomplaas Hill (Viglietti, 2016), with
655 overbank deposits (FA5), resulting from floodplain aggradation through suspension settling
656 of finer grained material and by deposition of crevasse splay deposits (Miall, 2006; Viglietti,
657 2016; Viglietti et al., 2018). Similarly, a high sinuosity fluvial style for the Balfour Formation
658 in the north-eastern Free State and KwaZulu-Natal, with river channels flanked by broad
659 floodplains, has previously been proposed (Turner, 1977; Groenewald, 1984, 1990; Green,
660 1997) and is supported by the abundance of LA elements (Figure 6). The predominance of
661 lithofacies type F1 (sometime associated with abundant leaf impressions), carbonaceous
662 mudstones, and even thin coal beds (lithofacies type C), provide evidence for the presence of
663 ponds/lakes and swampy conditions on the floodplain (Miall, 2006; Viglietti et al., 2018).

664 As noted earlier, the Balfour Formation in the southern Free State can be easily distinguished
665 from the underlying Abrahamskraal Formation based on the predominance of reddish
666 mudrocks. Reddish mudrocks are also present in the lower parts of the Beaufort Group in the
667 central Free State (Brandfort and Theunissen districts) but become less common towards the
668 north and east. In the vicinities of Virginia and Kroonstad, reddish mudrocks are absent from
669 the Balfour Formation and green grey and yellow grey mudrocks are predominant. A similar
670 situation is present in the north-eastern Free State and KwaZulu-Natal, with reddish
671 mudrocks entirely absent from the interval investigated during this study.

672 Reddish mudrocks have traditionally been cited as an indicator of increased aridity in
673 continental settings (Sheldon, 2005) and the increased abundance of reddish mudrocks in the
674 upper interval suggests a change in climatic conditions between the Abrahamskraal and
675 Balfour formations. This simplistic view is not always the case as mudrock colours are
676 influenced by oxidation and can be affected by several factors, including the level of the
677 water table at the time of deposition, hydrological drainage, and through diagenetic processes

678 (Miall, 1977; Sheldon, 2005; Wilson et al., 2014; Paiva, 2015; Li et al., 2017). Following the
679 conceptual model presented by Wilson *et al.* (2014), variations in the height of the water
680 table (shortly after deposition) drive the oxidation of iron, and thereby the colour of the
681 mudrocks. More drab colours indicate reducing conditions during higher water table
682 conditions, whereas redder colours indicate lower water tables that resulted in subaerial
683 exposure (Wilson et al., 2014).

684 The regional water table is considered a landward extension of the relative sea level in fluvial
685 sequence stratigraphy (Gulliford et al., 2014). As such, a change in base level would affect
686 the water table and the change in colouration may reflect the proximity to the coastline i.e.
687 the Balfour Formation in the southern part of the study area was deposited further from the
688 shoreline where the water table was subject to more rapid (seasonal?) fluctuations, resulting
689 in an increased abundance of reddish mudrocks. If, however, the colouration is the result of
690 climatic conditions, the abundance of reddish mudrocks in the upper interval may indicate
691 increased aridity with a lower water table and prolonged subaerial conditions (Wilson et al.,
692 2014). The presence of desiccation cracks and gypsum crystals are further indicators of
693 prolonged and repeated wetting and drying events that occur in subaerial and semi-arid
694 conditions (Smith, 1990, 1993).

695 The absence of reddish mudrocks from the studied interval of the Balfour Formation in the
696 north-eastern Free State and KwaZulu-Natal, suggests that the water table in this part of the
697 basin was relatively high and subject to little variation. A high water table is corroborated by
698 abundant soft-sediment deformation structures in the interval between the Waterford
699 Formation of the Ecca Group and Rooinek Member of the Balfour Formation. The higher
700 water table, at least in the lower parts of the Balfour Formation, may be associated with the
701 proximity to the shoreline. However, it is also plausible that the Balfour Formation in the
702 north-eastern part of the basin was deposited in a generally moist environment as a result of

703 the topographic effect of the Eastern Highlands. A similar mechanism was proposed by
704 Bordy and Prevec (2008) for the (likely) contemporaneous Emakwezini Formation.

705 5.2 Biostratigraphy

706 5.2.1 Biostratigraphy of the southern Free State

707 The lowest biozone present immediately above the Ecca-Beaufort contact in the southern
708 Free State is the *Eosimops–Glanosuchus* subzone of the *Tapinocephalus* AZ, and the rocks
709 are assigned to the Abrahamskraal Formation (Groenewald et al., 2019; Day and Rubidge,
710 2020; Groenewald, 2021). The northward thinning strata of the *Eosimops–Glanosuchus*
711 subzone can be followed northwards from the Orange River to the Fauresmith and
712 Jagersfontein districts, where this stratigraphic interval pinches out somewhere to the north of
713 the locality Vaalkop 695 near Jagersfontein (Groenewald et al., 2019; Day and Rubidge,
714 2020; Groenewald, 2021). While the immediately overlying strata are assigned to the Balfour
715 Formation (Viglietti, 2016; Groenewald, 2021), it is difficult to positively assign the faunal
716 assemblage to the upper *Cistecephalus* or lower *Daptocephalus* AZs. This is because faunas
717 of the uppermost *Cistecephalus* AZ and lower *Daptocephalus* AZ have many species in
718 common, including the dicynodonts *Aulacephalodon*, *Basilodon*, *Dinanomodon*, *Oudenodon*,
719 and *Diictodon* (Nicolas, 2007; Smith et al., 2012; Viglietti, 2016, 2020; Viglietti et al., 2016;
720 Smith, 2020), and none of the index fossils (*Cistecephalus microrhinus*, *Daptocephalus*
721 *leoniceps*, and *Therionathus microps*) have been recovered from this area to date. However,
722 because *Cistecephalus* has not been recovered from within the study area, but has been
723 recovered from several localities immediately south of the study area (Kitching, 1967, 1977),
724 most localities yielding *Oudenodon* north of the Orange River are assigned to the *Dicynodon-*
725 *Therionathus* subzone (Viglietti, 2016, 2020; Groenewald et al., 2019; Groenewald, 2021).
726 The potential exception to this is strata at the base of Boomplaas Hill (locality 2: Figure 2)
727 and along the ridges in the vicinity, which may include uppermost *Cistecephalus* AZ based

728 on the presence of the *Endothiodon* specimen BP/1/7962 (Groenewald et al., 2019;
729 Groenewald, 2021).

730 5.2.2 Biostratigraphy of the central and north-eastern Free State and KwaZulu-Natal
731 Kitching (1977) considered the locality Kranskraal to fall within either the upper
732 *Cistecephalus* AZ or *Daptocephalus* AZ, whereas Angielczyk and Kammerer (2017) assign it
733 to the lower *Daptocephalus* AZ (*Dicynodon-Theriognathus* subzone; Viglietti 2020). Based
734 on the presence of *Rhachiocephalus* and *Compsodon*, the absence of *Cistecephalus*, and in
735 contrast to Viglietti (2016, 2020), we consider the *Dicynodon-Theriognathus* subzone of the
736 *Daptocephalus* AZ to be present immediately above the Ecca-Beaufort contact near
737 Bloemfontein in the central Free State.

738 Viglietti (2016) considered the sandstones exposed on Tafelkop, Bloemfontein, the
739 equivalent to the “Musgrave Grit” exposed near Thaba ‘Nchu (Rutherford, 2009; Rutherford
740 et al., 2015) and assigned them to the *Lystrosaurus maccaigi-Moschorhinus* subzone of the
741 *Daptocephalus* AZ. Rutherford et al. (2015) point out that the Palingkloof Member, or its
742 equivalents, are not preserved near Thaba ‘Nchu, and the *Daptocephalus* AZ is therefore
743 disconformably overlain by the *Lystrosaurus declivis* AZ. This is similar to the situation
744 observed by Hancox et al. (2002) near Senekal.

745 Of the few tetrapod fossils recovered near to the Ecca-Beaufort contact between Brandfort
746 and Kroonstad in the central portion of the study area, the *Uranocentrodon* specimen
747 BP/1/8195 is stratigraphically most useful. This is because the stratigraphic range of
748 *Uranocentrodon* is restricted to the *Daptocephalus* AZ (Latimer et al., 2002; Damiani, 2004;
749 Tarailo, 2018). However, most of the known *Uranocentrodon* specimens were collected from
750 a single locality near the town Senekal in the Free State Province where the Permo-Triassic
751 boundary is considered to be absent and a hiatus of unknown duration exists between the

752 *Daptocephalus* AZ and overlying *Lystrosaurus declivis* AZ (Hancox et al., 2002; Latimer et
753 al., 2002). As such, the range of *Uranocentrodon* within the *Daptocephalus* AZ is uncertain
754 at this stage. The presence of the *Daptocephalus* AZ in the central part of the study area is
755 further supported by the co-occurrence of *Theriognathus microps*, *Oudenodon bainii*, and
756 *Aulacephalodon bainii* in an area between the towns of Excelsior and Verkeerdevlei.
757 However, since these taxa all have stratigraphic ranges that extend upwards through the
758 *Dicynodon-Theriognathus* subzone AZ into the lower *Lystrosaurus maccaigi-Moschorhinus*
759 subzone (Viglietti et al., 2016; Viglietti, 2020), it is uncertain which of the subzones of the
760 *Daptocephalus* AZ is present in this part of the basin immediately above the Ecca-Beaufort
761 contact.

762 In the eastern Free State and KwaZulu-Natal, rocks of the Balfour Formation (Normandien
763 Formation) can be confidently assigned to the late Permian (Lopingian) *Daptocephalus* AZ,
764 which is in agreement with previous work (Groenewald, 1989, 1990; van der Walt et al.,
765 2010; Rubidge et al., 2016; Viglietti, 2020). Since both *Rhachiocephalus* and
766 *Kitchinganomodon* have their upper ranges in the *Dicynodon-Theriognathus* subzone
767 (Viglietti et al., 2016; Viglietti, 2020), this subzone is considered to be present at the base of
768 the Beaufort Group in the north eastern Free State.

769 The first appearance datum of *Lystrosaurus maccaigi* is used to define the lower boundary of
770 the *Lystrosaurus maccaigi-Moschorhinus* subzone of the *Daptocephalus* AZ (Viglietti et al.,
771 2016; Viglietti, 2020) and the association of *Lystrosaurus* with *Daptocephalus* at the locality
772 Venus suggests that the *Lystrosaurus maccaigi-Moschorhinus* subzone is present from
773 approximately 7 m below the Schoondraai Member in the north-eastern Free State. This is
774 further supported by a very large gorgonopsian maxilla (BP/1/8205) from a clay-pebble lag at
775 the base of the second sandstone of the Schoondraai Member at the locality Cliffdale, which
776 may be the same species as the large gorgonopsians (e.g. NMQR 3707) reported from the

777 uppermost *Daptocephalus* AZ at Nooitgedacht 68 (Botha-Brink et al., 2014; Butler et al.,
778 2017), and the presence of a *Lystrosaurus declivis* AZ fauna in the overlying Harrismith
779 Member (Groenewald, 1990, 1996; Botha et al., 2020; Botha and Smith, 2020).

780 In KwaZulu-Natal, the presence of *Daptocephalus* and *Dicynodon* supports the presence of
781 the *Daptocephalus* AZ. Based on the current data, however, it is uncertain at this stage
782 whether the *Dicynodon-Theriongnathus* subzone is present near Estcourt. This is because most
783 of the vertebrate fossil yielding localities in the Estcourt District are in the upper portion of
784 the Balfour Formation. Although it is difficult to get an accurate thickness for the Balfour
785 Formation in this part of the basin (Botha and Linström, 1978), it is estimated that some of
786 these localities e.g. Oatesdale, are up to 150 m above the Ecca-Beaufort contact as defined by
787 this study. As such, it is possible that the lower *Daptocephalus* AZ is present in the Estcourt
788 district, but further collecting is required to confirm this. Oatesdale Quarry near Mooi River,
789 which is slightly higher in the stratigraphic succession, has yielded *Dicynodontoides* and a
790 gorgonopsian in association with *Lystrosaurus maccaigi*. Strata at this locality are therefore
791 confidently assigned to the latest Permian (Changhsingian) *Lystrosaurus maccaigi*-
792 *Moschorhinus* subzone (Viglietti et al., 2016; Viglietti, 2020).

793 5.3 Status of the Normandien Formation

794 On the 2019 1:1 M geological map (Council for Geoscience, 2019), the Normandien
795 Formation is included in the Balfour Formation of the Beaufort Group. As the Frankfort
796 Member, the lowermost stratigraphic unit of the Normandien Formation, (Groenewald, 1984,
797 1989), is here considered equivalent to the Waterford Formation, it should therefore be
798 included in the Ecca Group rather than the Beaufort Group. We propose that the Normandien
799 Formation in the northern Karoo Basin be replaced by the Balfour Formation. The arenaceous
800 Rooinek and Schoondraai members and argillaceous Harrismith Member (Groenewald, 1984,
801 1989) which are useful regional stratigraphic markers in the northern part of the Karoo Basin

802 (Muntingh, 1989; Claassen, 2008) should be retained and given formal status as members
803 within the Balfour Formation.

804 6 Conclusions

805 This study has demonstrated that the Waterford Formation of the Ecca Group, not previously
806 recognised in the distal sector of the Karoo Basin, is present throughout the study area and
807 includes strata currently mapped as both the uppermost Volksrust/Tierberg formations of the
808 Ecca Group and lowermost Adelaide Subgroup of the Beaufort Group. This has implications
809 for the mapped position of the Ecca-Beaufort contact which, we have demonstrated, should
810 coincide with the top of the Waterford Formation rather than the base of the first prominent
811 sandstone.

812 In the southern Free State Province, rocks of the lowermost Beaufort Group correlate with the
813 Abrahamskraal Formation based on biostratigraphy. Here the middle Permian Abrahamskraal
814 Formation is directly and unconformably overlain by rocks of the late Permian Balfour
815 Formation, which can be easily recognised by the predominance of reddish brown mudrock.

816 In the central and north-eastern Free State and KwaZulu-Natal, most of the mapped Frankfort
817 Member of the Normandien Formation (Groenewald, 1984, 1989, 1990) has been shown to
818 be lithologically the same as the Waterford Formation of the Ecca Group and thus it is
819 recommended that the term Normandien Formation no-longer be used. Rather, the remainder
820 of the Normandien Formation including the prominent arenaceous Rooinek and Schoondraai
821 members and argillaceous Harrismith Member, should be incorporated into the Balfour
822 Formation and these units should be given formal member status.

823 Extensive fossil collecting for this project, coupled with recent Karoo biostratigraphic
824 advancements (Smith et al., 2020), has enabled refined biostratigraphic determination of
825 lower Beaufort Group deposits in the distal parts of the main Karoo Basin. Based on the co-

826 occurrence of *Eosimops* and *Glanosuchus* in the southern Free State, it is apparent that,
827 contrary to previous understanding (Rubidge, 1995; van der Walt et al., 2010), the oldest
828 tetrapod biozone present in this part of the basin is the *Eosimops-Glanosuchus* subzone of the
829 *Tapinocephalus* AZ (Groenewald et al., 2019; Smith et al., 2020). Rocks immediately
830 overlying the *Tapinocephalus* AZ strata in the southern Free State host a tetrapod fossil fauna
831 characteristic of either the upper *Cistecephalus* AZ or lower *Daptocephalus* AZ (*Dicynodon-*
832 *Theriongnathus* subzone; Groenewald et al. 2019).

833 In the central and north-eastern Free State and in KwaZulu-Natal, the *Dicynodon-*
834 *Theriongnathus* subzone of the *Daptocephalus* AZ directly overlies the Waterford Formation
835 based on the presence of *Rhachiocephalus* and *Kitchinganomodon*. In turn it is overlain by
836 the *Lystrosaurus maccaigi-Moschorhinus* subzone of the *Daptocephalus* AZ. The first
837 appearance datum of *Lystrosaurus maccaigi*, which demarcates the lower boundary of the
838 *Lystrosaurus maccaigi-Moschorhinus* subzone (Viglietti, 2020), coincides roughly with the
839 Musgrave Grit and Schoondraai Member in the central and north-eastern Free State,
840 respectively.

841 This enhanced understanding of the bio- and lithostratigraphy of the northern (distal) sector
842 of the main Karoo Basin has important consequences for Karoo Basin development
843 modelling during the Permian. Of particular importance is an apparent ~6 Ma hiatus in the
844 southern Free State Province (Groenewald et al., 2019; Groenewald, 2021) and the out of
845 phase deposition of sandstone rich intervals in the Balfour Formation in the north versus the
846 south e.g. the Schoondraai and Ripplemead members (Viglietti et al., 2017a; Groenewald,
847 2021). The implications of these observations will be discussed in a future paper.

848 **Acknowledgements**

849 This work was made possible by financial support from the National Research Foundation
850 (NRF) and its African Origins Platform, the DSI-NRF Centre of Excellence in Palaeosciences
851 (CoE-Pal), the Palaeontological Scientific Trust (PAST), and the Geological Society of South
852 Africa’s Research, Education and Investment (REI) Fund. Conclusions arrived at, are not
853 necessarily to be attributed to the NRF or to the CoE-Pal. We thank the farmers and locals for
854 their hospitality and for allowing us access to their farms in order to prospect for and
855 excavate specimens, and to undertake geological investigations. We are grateful to the
856 preparators at the ESI (Charlton Dube, Gilbert Mokgethoa, Gladys Mokoma, Pepson
857 Mukunela, Thilivhali Nemavhundi and Wilfred Bilankulu). For their help in dealing with
858 existing collections, and with accessioning new material, we thank Bernhard Zipfel, Sifelani
859 Jirah, Jennifer Botha, Elize Butler, John Midgely, Matabaro Ziganira, and Nonhlanhla
860 Mchunu. Lastly, we thank the editors and reviewers, Michiel de Kock and John Hancox, for
861 their constructive comments and suggestions.

862 **References**

- 863 AHMED, S., BHATTACHARYA, J.P., GARZA, D.E., and LI, Y., 2014, Facies Architecture and
864 Stratigraphic Evolution of A River-Dominated Delta Front, Turonian Ferron
865 Sandstone, Utah, U.S.A: *Journal of Sedimentary Research*, v. 84, p. 97–121, doi:
866 10.2110/jsr.2014.6.
- 867 ANDERSON, A.M., 1975, Limulid Trackways in the Late Palaeozoic Ecca Sediments and their
868 Palaeoenvironmental Significance: *South African Journal of Science*, v. 71, p. 249–
869 251.
- 870 ANGIELCZYK, K.D., and KAMMERER, C.F., 2017, The cranial morphology, phylogenetic
871 position and biogeography of the upper Permian dicynodont *Compsodon helmoedi*
872 van Hoepen (Therapsida, Anomodontia): *Papers in Palaeontology*, v. 3, p. 513–545,
873 doi: 10.1002/spp2.1087.
- 874 AUGUSTINUS, P.G.E.F., 1989, Cheniers and chenier plains: A general introduction: *Marine*
875 *Geology*, v. 90, p. 219–229, doi: 10.1016/0025-3227(89)90126-6.
- 876 BARBOLINI, N., BAMFORD, M.K., and RUBIDGE, B., 2016, Radiometric dating demonstrates
877 that Permian spore-pollen zones of Australia and South Africa are diachronous:
878 *Gondwana Research*, v. 37, p. 241–251, doi: 10.1016/j.gr.2016.06.006.
- 879 BARS, H., and GUILLEBERT, P., 1976, Geological investigation of the Vrede-Memel-
880 Volksrust Area.: Geological Survey of South Africa (Council for Geoscience)
881 SOEKOR internal report 1976–0099, 12 p.
- 882 BEHOUNEK, N.J., 1980, The geology of an area west of Welkom, OFS: degree blocks 2825A
883 and B and 2826A: Unpublished MSc dissertation, University of the Orange Free
884 State, Bloemfontein, South Africa, 162 p.
- 885 BHATTACHARYA, J.P., 2010, Deltas, *in* James, N.P. and Dalrymple, R.W., eds., *Facies*
886 *Models 4: GEOText 6*, Geolog. Assoc. of Canada, St. Johns, p. 233–264.
- 887 BHATTACHARYA, J.P., and GIOSAN, L., 2003, Wave-influenced deltas: geomorphological
888 implications for facies reconstruction: *Sedimentology*, v. 50, p. 187–210, doi:
889 10.1046/j.1365-3091.2003.00545.x.
- 890 BHATTACHARYA, J.P., and MACEACHERN, J.A., 2009, Hyperpycnal Rivers and Prodeltaic
891 Shelves in the Cretaceous Seaway of North America: *Journal of Sedimentary*
892 *Research*, v. 79, p. 184–209, doi: 10.2110/jsr.2009.026.
- 893 BOJANOWSKI, M.J., and CLARKSON, E.N.K., 2012, Origin of Siderite Concretions In
894 Microenvironments of Methanogenesis Developed In A Sulfate Reduction Zone: An
895 Exception Or A Rule? *Journal of Sedimentary Research*, v. 82, p. 585–598, doi:
896 10.2110/jsr.2012.50.
- 897 BORDY, E.M., and PAIVA, F., 2021, Stratigraphic Architecture of the Karoo River Channels at
898 the End-Capitanian: *Frontiers in Earth Science*, v. 8, p. 521766, doi:
899 10.3389/feart.2020.521766.

- 900 BORDY, E.M., and PREVEC, R., 2008, Sedimentology, palaeontology and palaeo-
901 environments of the Middle (?) to Upper Permian Emakwezini Formation (Karoo
902 Supergroup, South Africa): South African Journal of Geology, v. 111, p. 429–458,
903 doi: 10.2113/gssajg.111.4.429.
- 904 BOTHA, J., HUTTENLOCKER, A.K., SMITH, R.M.H., PREVEC, R., VIGLIETTI, P.A., and
905 MODESTO, S.P., 2020, New geochemical and palaeontological data from the Permian-
906 Triassic boundary in the South African Karoo Basin test the synchronicity of
907 terrestrial and marine extinctions: Palaeogeography, Palaeoclimatology,
908 Palaeoecology, v. 540, p. 109467, doi: 10.1016/j.palaeo.2019.109467.
- 909 BOTHA, B.J.V., and LINSTRÖM, W., 1977, Palaeogeological and palaeogeographical aspects
910 of the upper part of the Karoo Sequence in North-Western Natal: Annals of the
911 Geological Survey of South Africa, v. 12, p. 177–192.
- 912 BOTHA, B.J.V., and LINSTRÖM, W., 1978, A note on the stratigraphy of the Beaufort Group in
913 north-western Natal: Transactions of the Geological Society of South Africa, v. 81, p.
914 35–40.
- 915 BOTHA, J., and SMITH, R.M.H., 2020, Biostratigraphy of the *Lystrosaurus declivis*
916 Assemblage Zone (Beaufort Group, Karoo Supergroup), South Africa: South African
917 Journal of Geology, v. 123, p. 207–216, doi: 10.25131/sajg.123.0015.
- 918 BOTHA-BRINK, J., HUTTENLOCKER, A.K., and MODESTO, S.P., 2014, Vertebrate
919 palaeontology of Nooitgedacht 68: a *Lystrosaurus maccaigi*-rich Permo-Triassic
920 Boundary locality in South Africa, in Kammerer, C.F., Angielczyk, K.D., and
921 Fröbisch, J., eds., Early Evolutionary History of the Synapsida: Springer, Dordrecht,
922 p. 289–304.
- 923 BROOM, R., 1937, A further contribution to our knowledge of the Fossil Reptiles of the
924 Karoo: Proceedings of the Zoological Society of London, v. 107, p. 299–318.
- 925 BUATOIS, L.A., and MÁNGANO, M.G., 2011, Ichnology: organism-substrate interactions in
926 space and time: Cambridge University Press, Cambridge, UK, 358 p.
- 927 BUTLER, E., BOTHA-BRINK, J., and ABDALA, F., 2017, A new gorgonopsian from the
928 uppermost *Daptocephalus* Assemblage Zone, Karoo Basin of South Africa:
929 Palaeontologia africana, v. 51, p. 49.
- 930 CADLE, A.B., CAIRNCROSS, B., CHRISTIE, A.D.M., and ROBERTS, D.L., 1993, The Karoo
931 Basin of South Africa: type basin for the coal-bearing deposits of southern Africa:
932 International Journal of Coal Geology, v. 23, p. 117–157, doi: 10.1016/0166-
933 5162(93)90046-D.
- 934 CADLE, A.B., and PROEDROU, P., 1975, A structural investigation of the Warden North Area:
935 Geological Survey of South Africa (Council for Geoscience) SOEKOR internal report
936 1975–0088, 13 p.
- 937 CAIRNCROSS, B., 2001, An overview of the Permian (Karoo) coal deposits of southern Africa:
938 Journal of African Earth Sciences, v. 33, p. 529–562, doi: 10.1016/S0899-
939 5362(01)00088-4.

- 940 CAIRNCROSS, B., BEUKES, N.J., COETZEE, L.L., and REHFELD, U., 2005, The Bivalve
 941 *Megadesmus* from the Permian Volksrust Shale Formation (Karoo Supergroup),
 942 northeastern Karoo Basin, South Africa: implications for late Permian Basin
 943 development: *South African Journal of Geology*, v. 108, p. 547–556.
- 944 CAIRNCROSS, B., and CADLE, A.B., 1988a, Depositional palaeoenvironments of the coal-
 945 bearing Permian Vryheid Formation in the east Witbank Coalfield, South Africa:
 946 *South African Journal of Geology*, v. 91, p. 1–17.
- 947 CAIRNCROSS, B., and CADLE, A.B., 1988b, Palaeoenvironmental control on coal formation,
 948 distribution and quality in the Permian Vryheid Formation, East Witbank Coalfield,
 949 South Africa: *International Journal of Coal Geology*, v. 9, p. 343–370, doi:
 950 10.1016/0166-5162(88)90031-6.
- 951 CATUNEANU, O., 2004, Retroarc foreland systems—evolution through time: *Journal of*
 952 *African Earth Sciences*, v. 38, p. 225–242, doi: 10.1016/j.jafrearsci.2004.01.004.
- 953 CATUNEANU, O., HANCOX, P.J., and RUBIDGE, B.S., 1998, Reciprocal flexural behaviour and
 954 contrasting stratigraphies: A new basin development model for the Karoo retroarc
 955 foreland system, South Africa: *Basin Research*, v. 10, p. 417–439, doi:
 956 10.1046/j.1365-2117.1998.00078.x.
- 957 CATUNEANU, O., WOPFNER, H., ERIKSSON, P.G., CAIRNCROSS, B., RUBIDGE, B.S., SMITH,
 958 R.M.H., and HANCOX, P.J., 2005, The Karoo basins of south-central Africa: *Journal*
 959 *of African Earth Sciences*, v. 43, p. 211–253.
- 960 CLAASSEN, M., 2008, A note on the biostratigraphic application of Permian plant fossils of
 961 the Normandien Formation (Beaufort Group, Northeastern Main Karoo Basin), South
 962 Africa: *South African Journal of Geology*, v. 111, p. 263–280, doi:
 963 10.2113/gssajg.111.2-3.263.
- 964 COLE, D.I., JOHNSON, M.R., and DAY, M.O., 2016, Lithostratigraphy of the Abrahamskraal
 965 Formation (Karoo Supergroup), South Africa: *South African Journal of Geology*, v.
 966 119, p. 415–424, doi: 10.2113/gssajg.119.2.415.
- 967 COLE, D.I., and WIPPLINGER, P.E., 2001, Sedimentology and molybdenum potential of the
 968 Beaufort Group in the main Karoo basin, South Africa: *Memoir, Geological Survey of*
 969 *South Africa*, v. 80, p. 225.
- 970 COLEMAN, J.M., and PRIOR, D.B., 1978, Submarine Landslides in the Mississippi River
 971 Delta: Coastal Studies Institute, Center for Wetland Resources, Louisiana State
 972 University Technical Report No. 263, 10 p.
- 973 COLEMAN, J.M., and PRIOR, D.B., 1982, Deltaic environments of deposition, *in* Scholle, P.A.
 974 and Spearing, D., eds., *Sandstone Depositional Environments*: American Association
 975 of Petroleum Geologists, Tulsa, USA, p. 99–149.
- 976 COLLINSON, J.M., and THOMPSON, D.B., 1989, *Sedimentary Structures*: U. Hyman, London,
 977 U.K., 207 p.

- 978 COLOMBERA, L., MOUNTNEY, N.P., and MCCAFFREY, W.D., 2012, A relational database for
979 the digitization of fluvial architecture: concepts and example applications: *Petroleum*
980 *Geoscience*, v. 18, p. 129–140.
- 981 COLOMBERA, L., MOUNTNEY, N.P., and MCCAFFREY, W.D., 2013, A quantitative approach to
982 fluvial facies models: Methods and example results: *Sedimentology*, v. 60, p. 1526–
983 1558, doi: 10.1111/sed.12050.
- 984 COUNCIL FOR GEOSCIENCE, 2019, Geological Map of the Republic of South Africa and the
985 Kingdoms of Lesotho and Swaziland. 1: 1 000 000 scale. *Compiled by:* de Beer, C. H.
986 Council for Geoscience, Pretoria, South Africa.: Council for Geoscience.
- 987 CSAKY, A.V., and WACHSMUTH, W., 1971, Stratigraphy and hydrocarbon potential of the
988 Dwyka, Ecca and Beaufort Groups in the Northern Karoo: Geological Survey of
989 South Africa (Council for Geoscience) SOEKOR internal report 1977–0099, 126 p.
- 990 DAMIANI, R.J., 2004, Temnospondyls from the Beaufort Group (Karoo Basin) of South
991 Africa and their Biostratigraphy: *Gondwana Research*, v. 7, p. 165–173, doi:
992 10.1016/S1342-937X(05)70315-4.
- 993 DASHTGARD, S.E., SNEDDEN, J.W., and MACEACHERN, J.A., 2015, Unbioturbated sediments
994 on a muddy shelf: Hypoxia or simply reduced oxygen saturation? *Palaeogeography,*
995 *Palaeoclimatology, Palaeoecology*, v. 425, p. 128–138, doi:
996 10.1016/j.palaeo.2015.02.033.
- 997 DAY, M.O., RAMEZANI, J., BOWRING, S.A., SADLER, P.M., ERWIN, D.H., ABDALA, F., and
998 RUBIDGE, B.S., 2015, When and how did the terrestrial mid-Permian mass extinction
999 occur? Evidence from the tetrapod record of the Karoo Basin, South Africa:
1000 *Proceedings of the Royal Society B: Biological Sciences*, v. 282, p. 20150834, doi:
1001 10.1098/rspb.2015.0834.
- 1002 DAY, M.O., and RUBIDGE, B.S., 2014, A brief lithostratigraphic review of the Abrahamskraal
1003 and Koonap formations of the Beaufort Group, South Africa : Towards a basin-wide
1004 stratigraphic scheme for the Middle Permian Karoo: *Journal of African Earth Science*,
1005 v. 100, p. 227–242, doi: 10.1016/j.jafrearsci.2014.07.001.
- 1006 DAY, M.O., and RUBIDGE, B.S., 2020, Biostratigraphy of the *Tapinocephalus* Assemblage
1007 Zone.: *South African Journal of Geology*, v. 123, p. 149–164.
- 1008 VAN DIJK, D.E., HOBDAI, D.K.H., and TANKARD, A.J., 1978, Permo-Triassic lacustrine
1009 deposits in the Eastern Karoo Basin, Natal, South Africa, *in* Matter, A. and Tucker,
1010 M.E., eds., *Modern and Ancient Lake Sediments: Proceedings of a Symposium Held*
1011 *at the H.C. Ørsted Institute, University of Copenhagen, 12-13 August 1977: Special*
1012 *publication - International Association of Sedimentologists 2, Blackwell Scientific;*
1013 *[distributed by] Halsted Press, Oxford : New York, p. 225–239.*
- 1014 DUMAS, S., and ARNOTT, R.W.C., 2006, Origin of hummocky and swaley cross-stratification
1015 - The controlling influence of unidirectional current strength and aggradation rate:
1016 *Geology*, v. 34, p. 1073–1076, doi: 10.1130/G22930A.1.
- 1017 EKDALE, A.A., BROMLEY, R.G., and PEMBERTON, S.G., 1984, *Ichnology: The Use of Trace*
1018 *Fossils in Sedimentology and Stratigraphy: SEPM (Society for Sedimentary*

- 1019 Geology), Oklahoma, 316 p. <https://pubs.geoscienceworld.org/books/book/1149/>.
1020 Checked April 2020.
- 1021 ELLIOTT, T., 1974, Interdistributary bay sequences and their genesis: *Sedimentology*, v. 21, p.
1022 611–622, doi: 10.1111/j.1365-3091.1974.tb01793.x.
- 1023 FIELDING, C.R., 2010, Planform and Facies Variability in Asymmetric Deltas: Facies
1024 Analysis and Depositional Architecture of the Turonian Ferron Sandstone in the
1025 Western Henry Mountains, South-Central Utah, U.S.A.: *Journal of Sedimentary*
1026 *Research*, v. 80, p. 455–479, doi: 10.2110/jsr.2010.047.
- 1027 GALLOWAY, W.E., 1975, Process framework for describing the morphologic and stratigraphic
1028 evolution of deltaic depositional systems, *in* Broussard, M.L., ed., *Deltas: Models for*
1029 *Exploration*: Houston Geological Society, Houston, Texas, U.S.A., p. 87–98.
- 1030 GANI, M.R., and BHATTACHARYA, J.P., 2007, Basic Building Blocks and Process Variability
1031 of a Cretaceous Delta: Internal Facies Architecture Reveals a More Dynamic
1032 Interaction of River, Wave, and Tidal Processes Than Is Indicated by External Shape:
1033 *Journal of Sedimentary Research*, v. 77, p. 284–302, doi: 10.2110/jsr.2007.023.
- 1034 GASTALDO, R.A., KAMO, S.L., NEVELING, J., GEISSMAN, J.W., BAMFORD, M., and LOOY,
1035 C.V., 2015, Is the vertebrate-defined Permian-Triassic boundary in the Karoo Basin,
1036 South Africa, the terrestrial expression of the end-Permian marine event? *Geology*, v.
1037 43, p. 939–942, doi: 10.1130/G37040.1.
- 1038 GASTALDO, R.A., KAMO, S.L., NEVELING, J., GEISSMAN, J.W., LOOY, C.V., and MARTINI,
1039 A.M., 2020, The base of the *Lystrosaurus* Assemblage Zone, Karoo Basin, predates
1040 the end-Permian marine extinction: *Nature Communications*, v. 11, p. 1428, doi:
1041 10.1038/s41467-020-15243-7.
- 1042 GREEN, D., 1997, Palaeoenvironments of the Estcourt Formation (Beaufort Groups),
1043 KwaZulu-Natal.: Unpublished MSc dissertation, University of KwaZulu-Natal,
1044 Durban, South Africa, 188 p.
- 1045 GREEN, A.N., and SMITH, A.M., 2012, Can ancient shelf sand ridges be mistaken for Gilbert-
1046 type deltas? Examples from the Vryheid Formation, Ecca Group, KwaZulu-Natal,
1047 South Africa: *Journal of African Earth Sciences*, v. 76, p. 27–33, doi:
1048 10.1016/j.jafrearsci.2012.08.001.
- 1049 GROENEWALD, G.H., 1984, Stratigrafie en sedimentologie van die Groep Beaufort in die
1050 Noordoos-Vrystaat: Unpublished MSc dissertation, Randse Afrikaanse Universiteit
1051 (University of Johannesburg), Johannesburg, South Africa, 174 p.
- 1052 GROENEWALD, G.H., 1987, Lithostratigraphic boundary of the Ecca and Beaufort Groups in
1053 the north eastern Orange Free State with special reference to the mappability of the
1054 units, *in* Symposium on Stratigraphic Problems Relating to the Ecca-Beaufort
1055 Contact: Pretoria, South Africa, p. 20–22.
- 1056 GROENEWALD, G.H., 1989, Stratigrafie en sedimentologie van die Groep Beaufort in die
1057 noordoos-Vrystaat: *Bulletin van die Geologiese Opname van Suid-Afrika*, v. 96, p.
1058 62.

- 1059 GROENEWALD, G.H., 1996, Stratigraphy and Sedimentology of the Tarkastad Subgroup,
1060 Karoo Supergroup of South Africa.: Unpublished PhD Thesis, University of Port
1061 Elizabeth (Nelson Mandela University), Port Elizabeth, South Africa, 460 p.
- 1062 GROENEWALD, G.H., 1990, The use of palaeontology in the correlation of lithostratigraphic
1063 units in the Beaufort Group, Karoo Sequence of South Africa: *Palaeontologia*
1064 *africana*, v. 27, p. 21–30.
- 1065 GROENEWALD, D.P., 2015, Tetrapod trackways and the Ecca-Beaufort contact in the Estcourt
1066 district: Unpublished Honours research project, University of the Witwatersrand,
1067 Johannesburg, South Africa, 54 p.
- 1068 GROENEWALD, D.P., 2021, A litho- and biostratigraphic analysis of the lower Beaufort Group
1069 in the distal sector of the main Karoo Basin, South Africa – implications for the
1070 depositional history of the distal foredeep to back-bulge basin: Unpublished PhD
1071 Thesis, University of the Witwatersrand, Johannesburg, South Africa, 438 p.
- 1072 GROENEWALD, D.P., DAY, M.O., and RUBIDGE, B.S., 2019, Vertebrate assemblages from the
1073 north-central Main Karoo Basin, South Africa, and their implications for mid-Permian
1074 biogeography: *Lethaia*, v. 52, p. 486–501, doi: 10.1111/let.12326.
- 1075 GULLIFORD, A.R., FLINT, S.S., and HODGSON, D.M., 2014, Testing Applicability of Models
1076 of Distributive Fluvial Systems or Trunk Rivers in Ephemeral Systems:
1077 Reconstructing 3-D Fluvial Architecture in the Beaufort Group, South Africa: *Journal*
1078 *of Sedimentary Research*, v. 84, p. 1147–1169, doi: 10.2110/jsr.2014.88.
- 1079 HANCOX, P.J., BRANDT, D., REIMOLD, W.U., KOEBERL, C., and NEVELING, J., 2002,
1080 Permian-Triassic boundary in the Northwest Karoo Basin: Current stratigraphic
1081 placement, implications for basin development models, and search for evidence of
1082 impact, *in* Special Paper 356: Catastrophic Events and Mass Extinctions: Impacts and
1083 Beyond: Geological Society of America, p. 429–444.
1084 <https://pubs.geoscienceworld.org/books/book/512/chapter/3801354/>. Checked
1085 November 2018.
- 1086 HANCOX, P.J., and GÖTZ, A.E., 2014, South Africa’s coalfields — A 2014 perspective:
1087 *International Journal of Coal Geology*, v. 132, p. 170–254, doi:
1088 10.1016/j.coal.2014.06.019.
- 1089 VAN HOEPEN, E.C.N., 1934, Oor die indeling van die Dicyodontoidae na aanleiding van
1090 nuwe vorme.: *Paleontologiese Navorsing van die Nasionale Museum*, v. 2, p. 67–101.
- 1091 JAMES, N.P., and DALRYMPLE, R.W., 2010, Facies models 4: Geological Association of
1092 Canada, St. Johns, 586 p.
- 1093 JOHNSON, M.R., 1976, Stratigraphy and Sedimentology of the Cape and Karoo Sequences in
1094 the Eastern Cape Province: Unpublished PhD Thesis, Rhodes University,
1095 Grahamstown, South Africa, 336 p.
- 1096 JOHNSON, M.R., 1987, The Ecca-Beaufort boundary: defining the options, *in* Symposium on
1097 Stratigraphic Problems Relating to the Ecca-Beaufort Contact: Pretoria, South Africa,
1098 p. 1–2.

- 1099 JOHNSON, M.R., VAN VUUREN, C.J., VISSER, J.N.J., COLE, D.I., WICKENS, H. de V.,
 1100 CHRISTIE, A.D.M., ROBERTS, D.L., and BRANDI, G., 2006, Sedimentary rocks of the
 1101 Karoo Supergroup, *in* Johnson, M.R., Anhaeusser, C.R., and Thomas, R.J., eds., *The*
 1102 *Geology of South Africa: Council for Geoscience, Pretoria, p. 461–499.*
- 1103 JORISSEN, E.L., DE LEEUW, A., VAN BAAK, C.G.C., MANDIC, O., STOICA, M., ABELS, H.A.,
 1104 and KRIJGSMAN, W., 2018, Sedimentary architecture and depositional controls of a
 1105 Pliocene river-dominated delta in the semi-isolated Dacian Basin, Black Sea:
 1106 *Sedimentary Geology*, v. 368, p. 1–23, doi: 10.1016/j.sedgeo.2018.03.001.
- 1107 KEYSER, A.W., and SMITH, R.M.H., 1979, Vertebrate Biozonation of the Beaufort Group
 1108 with special reference to the Western Karoo Basin.: *Annals of the Geological Survey*
 1109 *of South Africa*, v. 12, p. 1–35.
- 1110 KINGSLEY, C.S., and THERON, J.C., 1964, Palaeocurrent directions in arkose of the Beaufort
 1111 Series in the Orange Free State: *Annals of the Geological Survey of South Africa*, v.
 1112 3, p. 71–74.
- 1113 KITCHING, J.W., 1967, On the examination of the Beaufort beds within the flood area of the
 1114 Hendrik Verwoerd Dam, Orange River Project: *South African Journal of Science*, v.
 1115 63, p. 386.
- 1116 KITCHING, J.W., 1977, The distribution of the karroo vertebrate fauna: with special reference
 1117 to certain genera and the bearing of this distribution on the zoning of the Beaufort
 1118 Beds, Bernard Price Institute for Palaeontological Research, University of the
 1119 Witwatersrand: .
- 1120 KNAUST, D., and BROMLEY, R.G., 2012, Trace fossils as indicators of sedimentary
 1121 environments: Elsevier, Amsterdam, 924 p.
- 1122 LATIMER, E.M., HANCOX, P.J., RUBIDGE, B.S., SHISHKIN, M.A., and KITCHING, J.W., 2002,
 1123 The temnospondyl amphibian *Uranocentrodon*, another victim of the end-Permian
 1124 extinction event: *South African Journal of Science*, p. 191–193.
- 1125 LI, J., GASTALDO, R.A., NEVELING, J., and GEISSMAN, J.W., 2017, Siltstones across the
 1126 *Daptocephalus (Dicynodon)* and *Lystrosaurus* Assemblage Zones, Karoo Basin,
 1127 South Africa, show no evidence for aridification: *Journal of Sedimentary Research*, v.
 1128 87, p. 653–671, doi: 10.2110/jsr.2017.35.
- 1129 LINSTRÖM, W., 1973, Die geologie van die Sisteem Karoo wes van Mooirivier, Natal:
 1130 Unpublished MSc dissertation, Universiteit van die Oranje-Vrystaat, Bloemfontein,
 1131 94 p.
- 1132 LINSTRÖM, W., 1981, Die Geologie van die Gebied Drakensberg: Explanation of sheet 2928,
 1133 scale1: 250 000: Department of Mineral and Energy Affairs, Geological Survey of
 1134 South Africa, Pretoria, South Africa, 33 p.
- 1135 LINSTRÖM, W., 1987, Die Eccla/Beaufortkontak in sentraal- en suid-Natal, *in* Symposium on
 1136 Stratigraphic Problems Relating to the Eccla-Beaufort Contact: Pretoria, South Africa,
 1137 p. 23–24.

- 1138 LOOCK, J.C., and GROBLER, N.J., 1988, The regional geology of Florisbad: Navorsing van die
1139 Nationale Museum Bloemfontein, v. 5, p. 490–497.
- 1140 MACEachern, J.A., BANN, K.L., BHATTACHARYA, J.P., and HOWELL JR., C.D., 2005,
1141 Ichnology of deltas; organism responses to the dynamic interplay of rivers, waves,
1142 storms, and tides, *in* River Deltas - Concepts, Models, and Examples: SEPM Special
1143 Publication, Society for Sedimentary Geology, p. 1–36.
- 1144 MACEachern, J.A., PEMBERTON, S.G., GINGRAS, M.K., and BANN, K.L., 2010, Ichnology
1145 and Facies Models, *in* James, N.P. and Dalrymple, R.W., eds., Facies Models 4:
1146 GEOText 6, Geological Association of Canada, St. Johns, p. 19–58.
- 1147 MARSHALL, J.D., and PIRRIE, D., 2013, Carbonate concretions-explained: *Geology Today*, v.
1148 29, p. 53–62, doi: 10.1111/gto.12002.
- 1149 MASON, R., 2007, A bio- and litho-stratigraphic study of the Ecca-Beaufort Contact in the
1150 southeastern Karoo Basin (Albany District, Eastern Cape Province): Unpublished
1151 MSc dissertation, University of the Witwatersrand, Johannesburg, South Africa, 147
1152 p.
- 1153 MASON, R., RUBIDGE, B., and HANCOX, J., 2015, Terrestrial vertebrate colonisation and the
1154 Ecca- Beaufort boundary in the south-eastern main Karoo Basin , South Africa :
1155 implications for Permian basin evolution: *South African Journal of Geology*, v. 118,
1156 p. 145–156, doi: 10.2113/gssajg.118.2.145.
- 1157 MAVUSO, S.S., 2014, A bio- and litho-stratigraphic study of the northern Karoo Basin near
1158 Virginia: Unpublished Honours research project, University of the Witwatersrand,
1159 Johannesburg, South Africa, 62 p.
- 1160 MIALL, A.D., 1977, A review of the braided-river depositional environment: *Earth-Science*
1161 *Reviews*, v. 13, p. 1–62, doi: 10.1016/0012-8252(77)90055-1.
- 1162 MIALL, A.D., 1985, Architectural-Element Analysis: A New Method of Facies Analysis
1163 Applied to Fluvial Deposits: *Earth-Science Reviews*, v. 22, p. 261–308.
- 1164 MIALL, A.D., 1996, The geology of fluvial deposits: Sedimentary facies, basin analysis, and
1165 petroleum geology: Springer.
- 1166 MIALL, A.D., 2006, The geology of fluvial deposits: Springer, 582 p.
- 1167 MIALL, A.D., 2016, *Stratigraphy: A Modern Synthesis*: Springer, 454 p.
1168 <http://link.springer.com/10.1007/978-3-319-24304-7>. Checked April 2020.
- 1169 MOORE, D., 1966, Deltaic Sedimentation: *Earth-Science Reviews*, v. 1, p. 87–104.
- 1170 MOUNTAIN, E.D., 1946, The Geology of an area east of Grahamstown., *in* Explanation Sheet
1171 of the Geological Survey of South Africa: Geological Survey of South Africa, p. 136.
- 1172 MULDER, T., SYVITSKI, J.P.M., MIGEON, S., FAUGÈRES, J.-C., and SAVOYE, B., 2003, Marine
1173 hyperpycnal flows: initiation, behavior and related deposits. A review: *Marine and*
1174 *Petroleum Geology*, v. 20, p. 861–882, doi: 10.1016/j.marpetgeo.2003.01.003.

- 1175 MUNTINGH, D.J., 1989, Die Geologie van die Gebied Frankfort: Explanation of sheet 2728,
1176 scale1: 250 000: Department of Mineral and Energy Affairs, Geological Survey of
1177 South Africa, Pretoria, South Africa, 23 p.
- 1178 MUNTINGH, D.J., 1990, Die sedimentologie en stratigrafie van die Ecca-Beaufort oorgang in
1179 die noordoostelike gedeelte van die hoof karookom.: Unpublished MSc dissertation,
1180 Randse Afrikaanse Universiteit (University of Johannesburg), Johannesburg, South
1181 Africa, 143 p.
- 1182 MUNTINGH, D.J., 1997, Sedimentologie en stratigraphie van die Ecca-Beaufort-oorgang in
1183 die noordoostelike gedeelte van die hoof Karookom: Bulletin of the Geological
1184 Survey of South Africa, v. 121, p. 46.
- 1185 NANSON, G.C., and CROKE, J.C., 1992, A genetic classification of floodplains:
1186 Geomorphology, v. 4, p. 459–486, doi: 10.1016/0169-555X(92)90039-Q.
- 1187 NEVELING, J., 2004, Stratigraphic and sedimentological investigation of the contact between
1188 the *Lystrosaurus* and the *Cynognathus* assemblage zones (Beaufort Group: Karoo
1189 Supergroup): Bulletin of the Geological Survey of South Africa, v. 137, p. 164.
- 1190 NICOLAS, M., 2007, An assessment of vertebrate biodiversity changes through the Permo-
1191 Triassic Beaufort Group (Karoo Supergroup) of South Africa and its significance in
1192 terms of biological basin development, hiatus periods and extinction events:
1193 Unpublished PhD Thesis, University of the Witwatersrand, Johannesburg, 488 p.
- 1194 NICOLAS, M., and RUBIDGE, B.S., 2009, Assessing content and bias in South African Permo-
1195 Triassic Karoo tetrapod fossil collections: Palaeontologia africana, v. 44, p. 13–20.
- 1196 OLARIU, C., and BHATTACHARYA, J.P., 2006, Terminal Distributary Channels and Delta
1197 Front Architecture of River-Dominated Delta Systems: Journal of Sedimentary
1198 Research, v. 76, p. 212–233, doi: 10.2110/jsr.2006.026.
- 1199 OLARIU, C., BHATTACHARYA, J.P., XU, X., AIKEN, C.L.V., ZENG, X., and MCMECHAN, G.A.,
1200 2005, Integrated study of ancient delta front deposits using ground-penetrating radar,
1201 and three-dimensional photorealistic data: Cretaceous Panther Tongue Sandstone,
1202 Utah, U.S.A., in Giosan, L. and Bhattacharya, J.P., eds., River Deltas-Concepts,
1203 Models, and Examples: SEPM (Society for Sedimentary Geology).
1204 <http://sp.sepmonline.org/content/sepspecpub/sepspriv/1.toccontent/83>. Checked May
1205 2020.
- 1206 OLARIU, C., STEEL, R.J., and PETTER, A.L., 2010, Delta-front hyperpycnal bed geometry and
1207 implications for reservoir modeling: Cretaceous Panther Tongue delta, Book Cliffs,
1208 Utah: AAPG Bulletin, v. 94, p. 819–845, doi: 10.1306/11020909072.
- 1209 PAIVA, F., 2015, Fluvial facies architecture and provenance history of the Abrahamskraal-
1210 Teekloof Formation transition (Lower Beaufort Group) in the main Karoo Basin.:
1211 Unpublished MSc dissertation, University of Cape Town, Cape Town, 98 p.
- 1212 PENN-CLARKE, C.R., RUBIDGE, B.S., and JINNAH, Z.A., 2019, Eifelian–Givetian (Middle
1213 Devonian) high-paleolatitude storm- and wave-dominated shallow-marine
1214 depositional systems from the Bidouw Subgroup (Bokkeveld Group) of South Africa:
1215 Journal of Sedimentary Research, v. 89, p. 1140–1170, doi: 10.2110/jsr.2019.61.

- 1216 PETTER, A.L., and STEEL, R.J., 2006, Hyperpycnal flow variability and slope organization on
 1217 an Eocene shelf margin, Central Basin, Spitsbergen: AAPG Bulletin, v. 90, p. 1451–
 1218 1472, doi: 10.1306/04240605144.
- 1219 PLATT, N.H., and KELLER, B., 1992, Distal alluvial deposits in a foreland basin setting-the
 1220 Lower Freshwater Miocene), Switzerland: sedimentology, architecture and
 1221 palaeosols: Sedimentology, v. 39, p. 545–565, doi: 10.1111/j.1365-
 1222 3091.1992.tb02136.x.
- 1223 PLINK-BJÖRKLUND, P., and STEEL, R.J., 2004, Initiation of turbidity currents: outcrop
 1224 evidence for Eocene hyperpycnal flow turbidites: Sedimentary Geology, v. 165, p.
 1225 29–52, doi: 10.1016/j.sedgeo.2003.10.013.
- 1226 PLINT, A.G., 2010, Wave- and storm-dominated shoreline and shallow marine systems, *in*
 1227 James, N.P. and Dalrymple, R.W., eds., Facies Models 4: GEOText 6, Geolog. Assoc.
 1228 of Canada, St. Johns, p. 167–199.
- 1229 RAMMUTLA, R.T., 2016, Lithofacies, Paleontology and Paleoenvironments of the Ecca-
 1230 Beaufort Contact in the north eastern Karoo Basin: Unpublished Honours research
 1231 project, University of the Witwatersrand, Johannesburg, South Africa, 39 p.
- 1232 RETALLACK, G.J., 1990, Soils of the past: an introduction to paleopedology: Unwin Hyman,
 1233 London, U.K., 520 p.
- 1234 RETALLACK, G.J., 2001, Soils of the past: an introduction to paleopedology: Blackwell
 1235 Science, Oxford ; Malden, MA, 404 p.
- 1236 ROGERS, A.W., DU TOIT, A.L., and BROOM, R., 1909, An introduction to the geology of Cape
 1237 Colony: Longmans, Green and co., London, U.K., 491 p.
- 1238 RUBIDGE, B.S., 1988, A palaeontological and palaeoenvironmental synthesis of the Permian
 1239 Ecca-Beaufort contact between Prince Albert and Rietbron, Cape Province, South
 1240 Africa: Unpublished PhD Thesis, University of Port Elizabeth (Nelson Mandela
 1241 University), Port Elizabeth, South Africa, 347 p.
- 1242 RUBIDGE, B.S., 1995, Biostratigraphy of the Beaufort Group (Karoo Supergroup)., *in*
 1243 Rubidge, B.S., ed., South African Committee for Stratigraphy. Biostratigraphic
 1244 Series, Council for Geoscience, Pretoria.
- 1245 RUBIDGE, B.S., 2005, Re-uniting lost continents - Fossil reptiles from the ancient Karoo and
 1246 their wanderlust: South African Journal of Geology, v. 108, p. 135–172, doi:
 1247 10.2113/108.1.135.
- 1248 RUBIDGE, B.S., and DAY, M.O., 2020, Biostratigraphy of the *Eodicynodon* Assemblage Zone
 1249 (Beaufort Group, Karoo Supergroup), South Africa: South African Journal of
 1250 Geology, v. 123, p. 141–148, doi: 10.25131/sajg.123.0010.
- 1251 RUBIDGE, B.S., DAY, M.O., BARBOLINI, N., HANCOX, P.J., CHOINIERE, J.N., BAMFORD,
 1252 M.K., VIGLIETTI, P.A., MCPHEE, B.W., and JIRAH, S., 2016, Advances in Nonmarine
 1253 Karoo Biostratigraphy: Significance for Understanding Basin Development, *in* Linol,
 1254 B. and de Wit, M.J., eds., Origin and Evolution of the Cape Mountains and Karoo

- 1255 Basin: Springer International Publishing, p. 141–149.
 1256 http://link.springer.com/10.1007/978-3-319-40859-0_14. Checked January 2020.
- 1257 RUBIDGE, B.S., DAY, M.O., VIGLIETTI, P.A., and ABDALA, F., 2015, *Priesterognathus*
 1258 Assemblage Zone fauna from the Central Free State Province – Support for reciprocal
 1259 stratigraphy in Karoo Basin Development.: *Palaeontologia africana*, v. 49, p. 105.
- 1260 RUBIDGE, B.S., ERWIN, D.H., RAMEZANI, J., BOWRING, S.A., and DE KLERK, W.J., 2013,
 1261 High-precision temporal calibration of Late Permian vertebrate biostratigraphy: U-Pb
 1262 zircon constraints from the Karoo Supergroup, South Africa: *Geology*, v. 41, p. 363–
 1263 366.
- 1264 RUBIDGE, B.S., HANCOX, P.J., and CATUNEANU, O., 2000, Sequence Analysis of the Ecca
 1265 Beaufort contact in the Southern Karoo: *South African Journal of Geology*, v. 103, p.
 1266 81–96.
- 1267 RUBIDGE, B.S., HANCOX, P.J., and MASON, R., 2012, Waterford Formation in the south-
 1268 eastern Karoo: Implications for basin development: *South African Journal of Science*,
 1269 v. 108, p. 3–7, doi: 10.4102/sajs.v108i3/4.829.
- 1270 RUST, I.C., SHONE, R.W., and SIEBRITS, L.B., 1991, Carnarvon Formasie: golf-oorheersde
 1271 sedimentasie in 'n vlak Karoosee: *South African Journal of Science*, v. 87, p. 198–
 1272 202.
- 1273 RUTHERFORD, A.B., 2009, The Sedimentology and Stratigraphy of the Beaufort Group of the
 1274 Karoo Supergroup in the Vicinity of Thaba Nchu, Central Free State Province:
 1275 Unpublished MSc dissertation, University of the Witwatersrand, Johannesburg, South
 1276 Africa, 252 p.
- 1277 RUTHERFORD, A.B., RUBIDGE, B.S., and HANCOX, P.J., 2015, Sedimentology and
 1278 Palaeontology of the Beaufort Group in the Free State Province Supports A
 1279 Reciprocal Foreland Basin Model for the Karoo Supergroup, South Africa: *South*
 1280 *African Journal of Geology*, v. 118, p. 355–372, doi: 10.2113/gssaj.118.4.355.
- 1281 RYAN, P.J., 1967, Stratigraphic and palaeocurrent analysis of the Ecca Series and the
 1282 lowermost Beaufort beds in the Karroo Basin of South Africa: Unpublished PhD
 1283 Thesis, University of the Witwatersrand, Johannesburg, South Africa, 210 p.
- 1284 SACS, 1980, Stratigraphy of South Africa: Handbook 8 (L. E. Kent, Ed.): Geological Survey
 1285 of South Africa, 690 p.
- 1286 SCHUTTE, I.C., 1993, Die Geologie van die Gebied Kroonstad: toeligting van blad 2226, skaal
 1287 1: 250 000: Departement van Mineral-en Energiesake, Geologiese Opname.
- 1288 SCHWARZ, E.H.L., 1896, Summary of the work done in the Tulbagh and Worcester District:
 1289 Annual Report of the Geological Commission of the Cape of Good Hope, v. 1, p. 27–
 1290 30.
- 1291 SEILACHER, A., 2007, Trace fossil analysis: Springer, Berlin, 226 p.
- 1292 SELOVER, R.W., and GASTALDO, R.A., 2005, A reinterpretation of the Wagendrift Quarry,
 1293 Estcourt, KwaZulu-Natal Province, and its implications for Karoo Basin

- 1294 Paleogeography: South African Journal of Geology, v. 108, p. 429–438, doi:
1295 10.2113/108.3.429.
- 1296 SHANMUGAM, G., 2006, Deep-Water Processes and Facies Models: Implications for
1297 Sandstone Petroleum Reservoirs: Elsevier, Amsterdam, The Netherlands, 476 p.
- 1298 SHELDON, N.D., 2005, Do red beds indicate paleoclimatic conditions?: A Permian case study:
1299 Palaeogeography, Palaeoclimatology, Palaeoecology, v. 228, p. 305–319, doi:
1300 10.1016/j.palaeo.2005.06.009.
- 1301 SIEBRITS, L.B., 1987, Die Formasie Carnarvon in die Carnarvongebied, *in* Symposium on
1302 Stratigraphic Problems Relating to the Ecca-Beaufort Contact: Pretoria, South Africa,
1303 p. 11.
- 1304 SMITH, R.M.H., 1990, Alluvial Paleosols and Pedofacies Sequences in the Permian Lower
1305 Beaufort of the Southwestern Karoo Basin, South Africa: Journal of Sedimentary
1306 Petrology, v. 60, p. 258–276, doi: 10.1306/212F916A-2B24-11D7-
1307 8648000102C1865D.
- 1308 SMITH, R.M.H., 1993, Sedimentology and Ichnology of Floodplain Paleosurfaces in the
1309 Beaufort Group (Late Permian), Karoo Sequence, South Africa: PALAIOS, v. 8, p.
1310 339–357, doi: 10.2307/3515265.
- 1311 SMITH, R.M.H., 2020, Biostratigraphy of the *Cistecephalus* Assemblage Zone.: South African
1312 Journal of Geology, v. 123, p. 181–190.
- 1313 SMITH, R.M.H., and BOTHA-BRINK, J., 2014, Anatomy of a mass extinction:
1314 Sedimentological and taphonomic evidence for drought-induced die-offs at the
1315 Permo-Triassic boundary in the main Karoo Basin, South Africa: Palaeogeography,
1316 Palaeoclimatology, Palaeoecology, v. 396, p. 99–118, doi:
1317 10.1016/j.palaeo.2014.01.002.
- 1318 SMITH, R.M.H., ERIKSSON, P.G., and BOTHA, W.J., 1993, A review of the stratigraphy and
1319 sedimentary environments of the Karoo-aged basins of Southern Africa: Journal of
1320 African Earth Science, v. 16, p. 143–169.
- 1321 SMITH, R.M.H., RUBIDGE, B.S., DAY, M.O., and BOTHA, J., 2020, Introduction to the
1322 tetrapod biozonation of the Karoo Supergroup: South African Journal of Geology, v.
1323 123, p. 131–140, doi: 10.25131/sajg.123.0009.
- 1324 SMITH, R., RUBIDGE, B., and VAN DER WALT, M., 2012, Therapsid biodiversity patterns and
1325 paleoenvironments of the Karoo Basin, South Africa, *in* Chinsamy-Turan, A., ed.,
1326 Forerunners of Mammals: Indiana University Press Indianapolis, Indiana, p. 31–64.
- 1327 TARAİLO, D.A., 2018, Taxonomic and ecomorphological diversity of temnospondyl
1328 amphibians across the Permian-Triassic boundary in the Karoo Basin (South Africa):
1329 Journal of Morphology, v. 279, p. 1840–1848, doi: 10.1002/jmor.20906.
- 1330 TAVENER-SMITH, R., COOPER, J.A.G., and RAYNER, R.J., 1988, Depositional environments in
1331 the Volksrust Formation (Permian) in the Mhlatuze River, Zululand: South African
1332 Journal of Geology, v. 91, p. 198–206.

- 1333 TERBLANCHE, J.C., 1979, Die geologie van 'n gebied oos van Carnarvon: Unpublished MSc
1334 dissertation, University of the Orange Free State, Bloemfontein, South Africa, 161 p.
- 1335 THERON, J.C., 1970, Some geological aspects of the Beaufort Series in the Orange Free State:
1336 Unpublished D.Sc Thesis, University of the Orange Free State, Bloemfontein, South
1337 Africa, 244 p.
- 1338 TURNER, J.R., 1977, Palaeoenvironmental study of the lower Beaufort in the northeast Karoo
1339 Basin: Unpublished MSc thesis, University of KwaZulu-Natal, Pietermaritzburg,
1340 South Africa, 138 p.
- 1341 TYE, R.S., and KOSTERS, E.C., 1986, Styles of interdistributary basin sedimentation:
1342 Mississippi delta plain, Louisiana: Transactions of the Gulf Coast Association of
1343 Geological Societies, v. 36, p. 575–588.
- 1344 VAN VUUREN, C.J., and COLE, D.I., 1979, The stratigraphy and depositional environments of
1345 the Ecca Group in the northern part of the Karoo Basin: Some Sedimentary Basins
1346 and Associated Ore Deposits of South Africa. Special Publication of the Geological
1347 Society of South Africa, v. 6, p. 103–111.
- 1348 VEEVERS, J.J., COLE, D.I., and COWAN, E.J., 1994, Southern Africa: Karoo Basin and Cape
1349 Fold Belt, *in* Geological Society of America Memoirs: Geological Society of
1350 America, p. 223–280.
1351 <https://pubs.geoscienceworld.org/books/book/191/chapter/3793611/>. Checked April
1352 2020.
- 1353 VIGLIETTI, P.A., 2016, Stratigraphy and sedimentary environments of the late Permian
1354 *Dicynodon* Assemblage Zone (Karoo Supergroup, South Africa) and implications for
1355 basin development.: Unpublished PhD Thesis, University of the Witwatersrand,
1356 Johannesburg, South Africa, 272 p.
- 1357 VIGLIETTI, P.A., 2020, Biostratigraphy of the *Daptocephalus* Assemblage Zone.: South
1358 African Journal of Geology, v. 123, p. 191–206.
- 1359 VIGLIETTI, P.A., BENSON, R.B.J., SMITH, R.M.H., BOTHA, J., KAMMERER, C.F., SKOSAN, Z.,
1360 BUTLER, E., CREAN, A., ELOFF, B., KAAL, S., MOHOI, J., MOLEHE, W., MTALANA, N.,
1361 MTUNGATA, S., et al., 2021, Evidence from South Africa for a protracted end-Permian
1362 extinction on land: Proceedings of the National Academy of Sciences, v. 118, p.
1363 e2017045118, doi: 10.1073/pnas.2017045118.
- 1364 VIGLIETTI, P.A., RUBIDGE, B.S., and SMITH, R.M.H., 2017a, New Late Permian tectonic
1365 model for South Africa's Karoo Basin: foreland tectonics and climate change before
1366 the end-Permian crisis: Scientific Reports, v. 7, p. 10861, doi: 10.1038/s41598-017-
1367 09853-3.
- 1368 VIGLIETTI, P.A., RUBIDGE, B.S., and SMITH, R.M.H., 2017b, Revised lithostratigraphy of the
1369 Upper Permian Balfour and Teekloof formations of the main Karoo Basin, South
1370 Africa: South African Journal of Geology, v. 120, p. 45–60.
- 1371 VIGLIETTI, P.A., SMITH, R.M.H., ANGIELCZYK, K.D., KAMMERER, C.F., FRÖBISCH, J., and
1372 RUBIDGE, B.S., 2016, The *Daptocephalus* Assemblage Zone (Lopingian), South
1373 Africa: A proposed biostratigraphy based on a new compilation of stratigraphic

- 1374 ranges: *Journal of African Earth Sciences*, v. 113, p. 153–164, doi:
1375 10.1016/j.jafrearsci.2015.10.011.
- 1376 VIGLIETTI, P.A., SMITH, R.M.H., and RUBIDGE, B.S., 2018, Changing palaeoenvironments
1377 and tetrapod populations in the *Daptocephalus* Assemblage Zone (Karoo Basin, South
1378 Africa) indicate early onset of the Permo-Triassic mass extinction: *Journal of African*
1379 *Earth Sciences*, v. 138, p. 102–111, doi: 10.1016/j.jafrearsci.2017.11.010.
- 1380 VILJOEN, J.H.A., 2005, Tierberg Formation. South African Committee for Stratigraphy, *in*
1381 Johnson, M.R., ed., *Catalogue of South African Lithostratigraphic Units.*: South
1382 African Committee for Stratigraphy, Pretoria, South Africa, p. 8–37.
- 1383 WALKER, R.G., and JAMES, N.P. (eds.), 1992, *Facies models: response to sea level change:*
1384 *Geological Association of Canada*, 409 p.
- 1385 VAN DER WALT, M., DAY, M., RUBIDGE, B., COOPER, A.K., and NETTERBERG, I., 2010, A
1386 new GIS-based biozone map of the Beaufort Group (Karoo Supergroup), South
1387 Africa: *Palaeontologia africana*, v. 45, p. 1–5.
- 1388 WELMAN, J., LOOCK, J.C., and RUBIDGE, B.S., 2001, New evidence for diachroneity of the
1389 Ecca-Beaufort contact (Karoo Supergroup, South Africa): *South African Journal of*
1390 *Science*, v. 97, p. 320–322.
- 1391 WILSON, A., FLINT, S., PAYENBERG, T., TOHVER, E., and LANCI, L., 2014, Architectural
1392 Styles and Sedimentology of the Fluvial Lower Beaufort Group, Karoo Basin, South
1393 Africa: *Journal of Sedimentary Research*, v. 84, p. 326–348, doi: 10.2110/jsr.2014.28.
- 1394 WRIGHT, L.D., 1977, *Sediment transport and deposition at river mouths: A synthesis:*
1395 *Geological Society of America Bulletin*, v. 88, p. 857–868.
- 1396 WRIGHT, V.P., and MARRIOTT, S.B., 1993, The sequence stratigraphy of fluvial depositional
1397 systems: the role of floodplain sediment storage: *Sedimentary Geology*, v. 86, p. 203–
1398 210, doi: 10.1016/0037-0738(93)90022-W.
- 1399 ZAWADA, P.K., 1987a, An evaluation of four possible positions for the Ecca-Beaufort contact
1400 in the S.W. Orange Free State, *in* *Symposium on Stratigraphic Problems Relating to*
1401 *the Ecca-Beaufort Contact: Pretoria, South Africa*, p. 18–19.
- 1402 ZAWADA, P.K., 1987b, *The stratigraphy and sedimentology of the Ecca and Beaufort Groups*
1403 *in the Fauresmith area.: Unpublished MSc dissertation, University of the*
1404 *Witwatersrand, Johannesburg, South Africa*, 192 p.
- 1405 ZAWADA, P.K., 1988a, *The Stratigraphy and sedimentology of the Ecca and Beaufort Groups*
1406 *in the Fauresmith area, south-western Orange Free State: Bulletin of the Geological*
1407 *Survey*, v. 90, p. 48.
- 1408 ZAWADA, P.K., 1988b, *Trace elements as possible palaeosalinity indicators for the Ecca and*
1409 *Beaufort Group mudrocks in the southwestern Orange Free State: South African*
1410 *Journal of Geology*, v. 91, p. 18–26.

1411 ZAWADA, P.K., and CADLE, A.B., 1988, Position of the Ecca-Beaufort contact in the
1412 southwestern Orange Free State: an evaluation of four possible alternatives: South
1413 African Journal of Geology, v. 91, p. 49–56.

1414

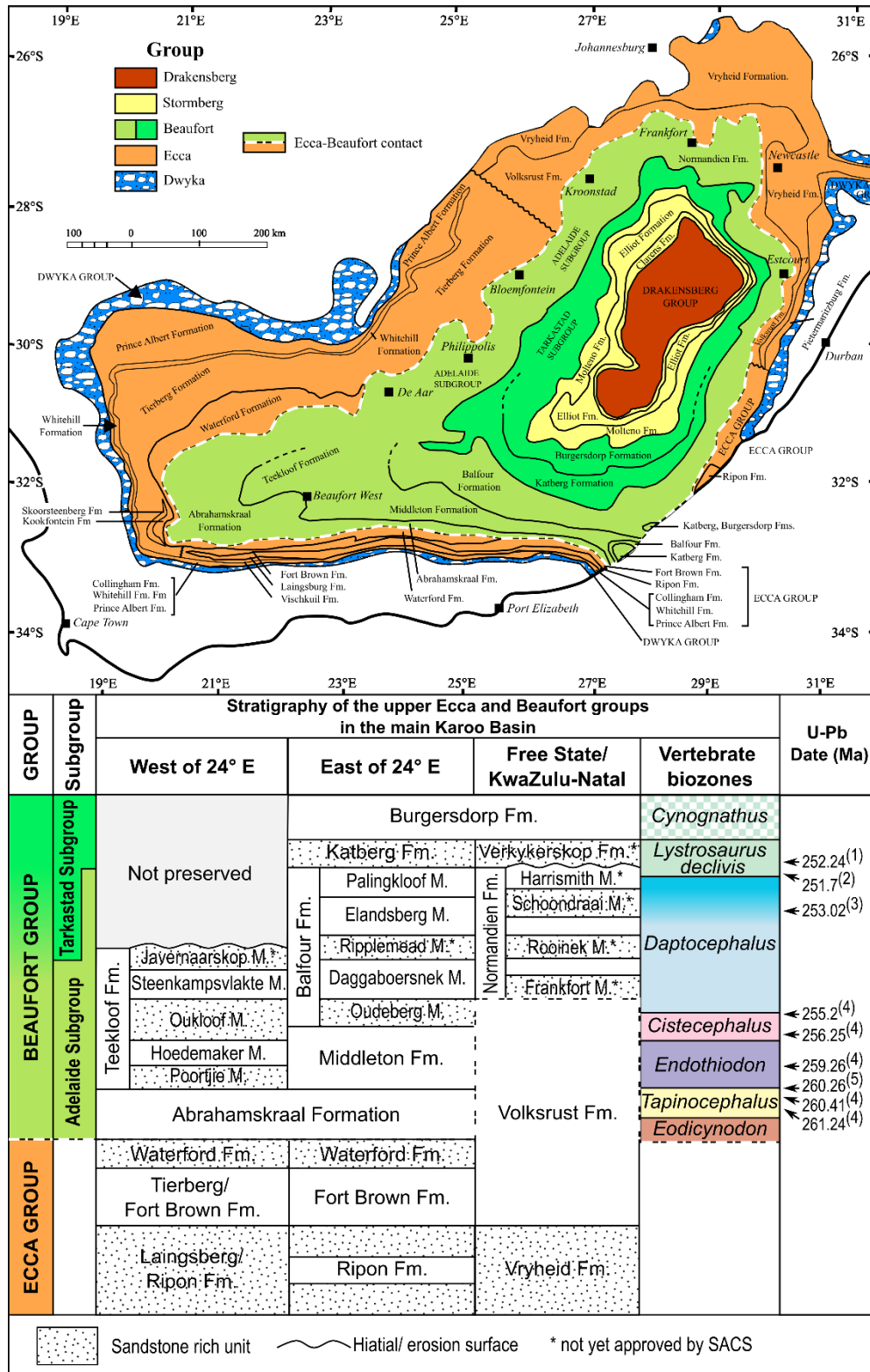


Figure 1 Simplified geological map of the main Karoo Basin and table reflecting the present understanding of the stratigraphy of the upper Ecca and Beaufort groups in the different portions of the basin. Map modified from Catuneanu et al. (2005). Members of the Abrahamskraal Formation are not shown, and thicknesses of stratigraphic units are not to scale. Subdivisions of biozones are also not shown. Biozone colours correspond to those in Figure 2. Fm. = Formation; M. = Member. Table modified from Barbolini et al. (2016) with additional data from Viglietti (2016), Cole et al. (2016), and Smith et al. (2020). Sources for radiometric ages: (1) Gastaldo et al. (2020); (2) Botha et al. (2020); (3) Gastaldo et al. (2015); (4) Rubidge et al. (2013); (5) Day et al. (2015).

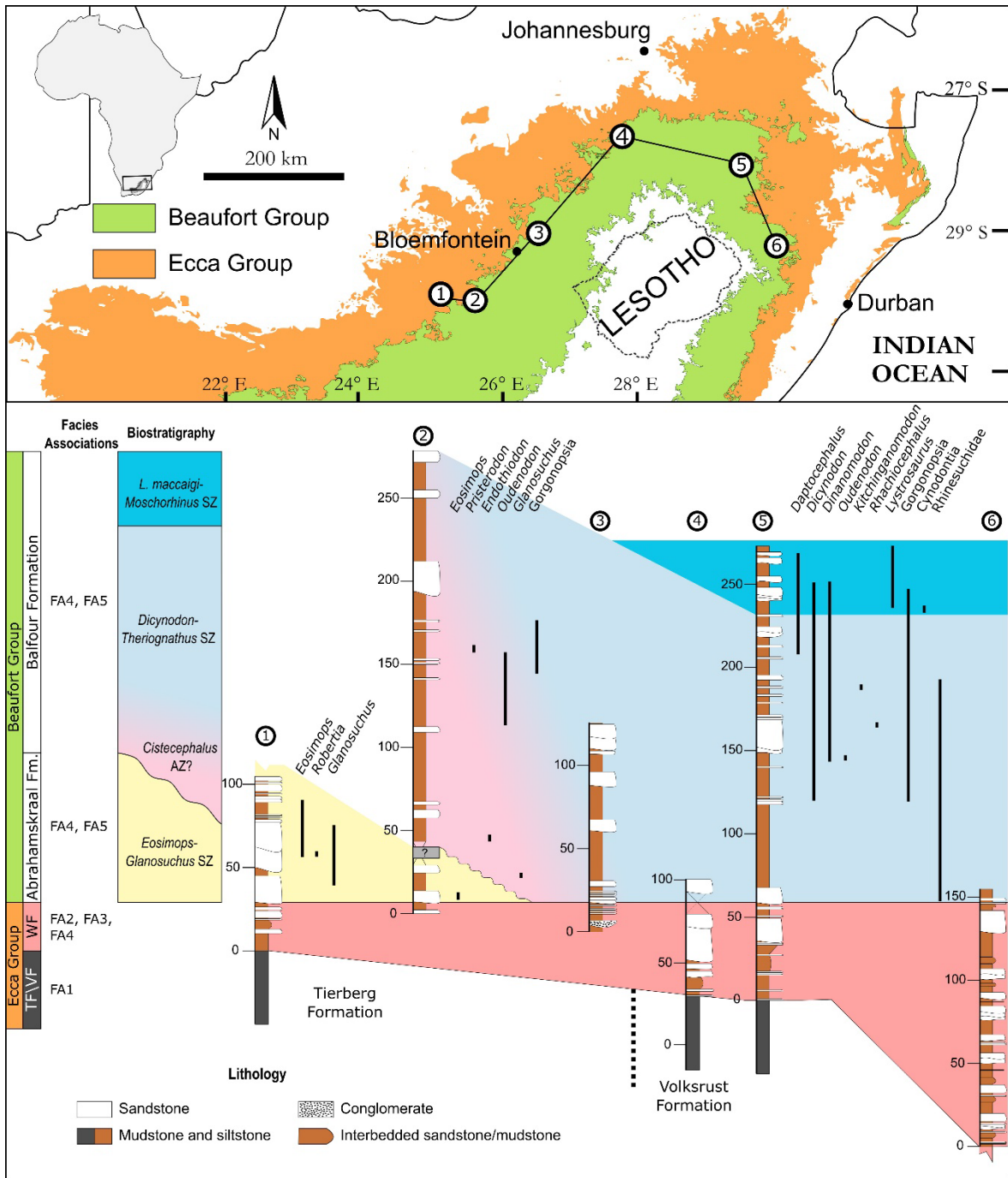


Figure 2 Fence diagram of six composite stratigraphic sections across the study area, highlighting the difference in thicknesses of stratigraphic units throughout the northern part of the main Karoo Basin, and showing the stratigraphic ranges of collected vertebrate fossils. Positions of stratigraphic sections numbered 1-6 are shown in the overview map. Localities: (1) Sandymount Park; (2) Jagersfontein; (3) Brandfort; (4) Borehole J.82/6; (5) North-eastern Free State; (6) Van der Merwe’s Kraal, Estcourt. AZ = Assemblage Zone; SZ = subzone; TF = Tierberg Formation; VF = Volksrust Formation; WF = Waterford Formation. The shading between the *Cistecephalus* AZ? and the *Dicynodon-Theriognathus* SZ (*Daptocephalus* AZ) reflects the uncertainty surrounding the presence and placement of the contact between the two zones in this part of the basin.

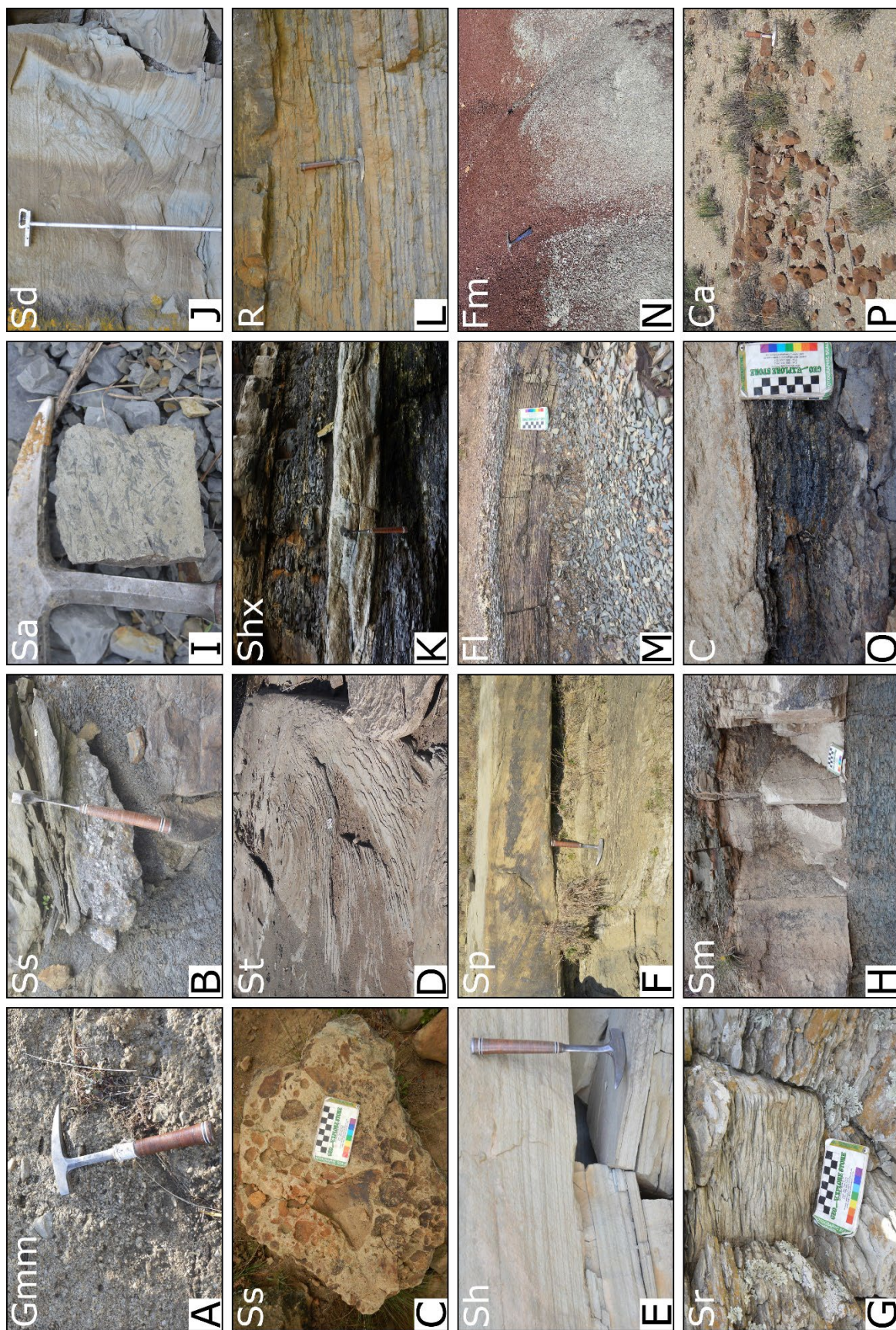


Figure 3 Field photographs showing examples of lithofacies types Gmm, Ss, St, Sh, Sp, Sr, Sm, Sa, Sd, Shx, R, Fl, Fm, C, and Ca in the study area. See Table 1 for more details of each lithofacies type.

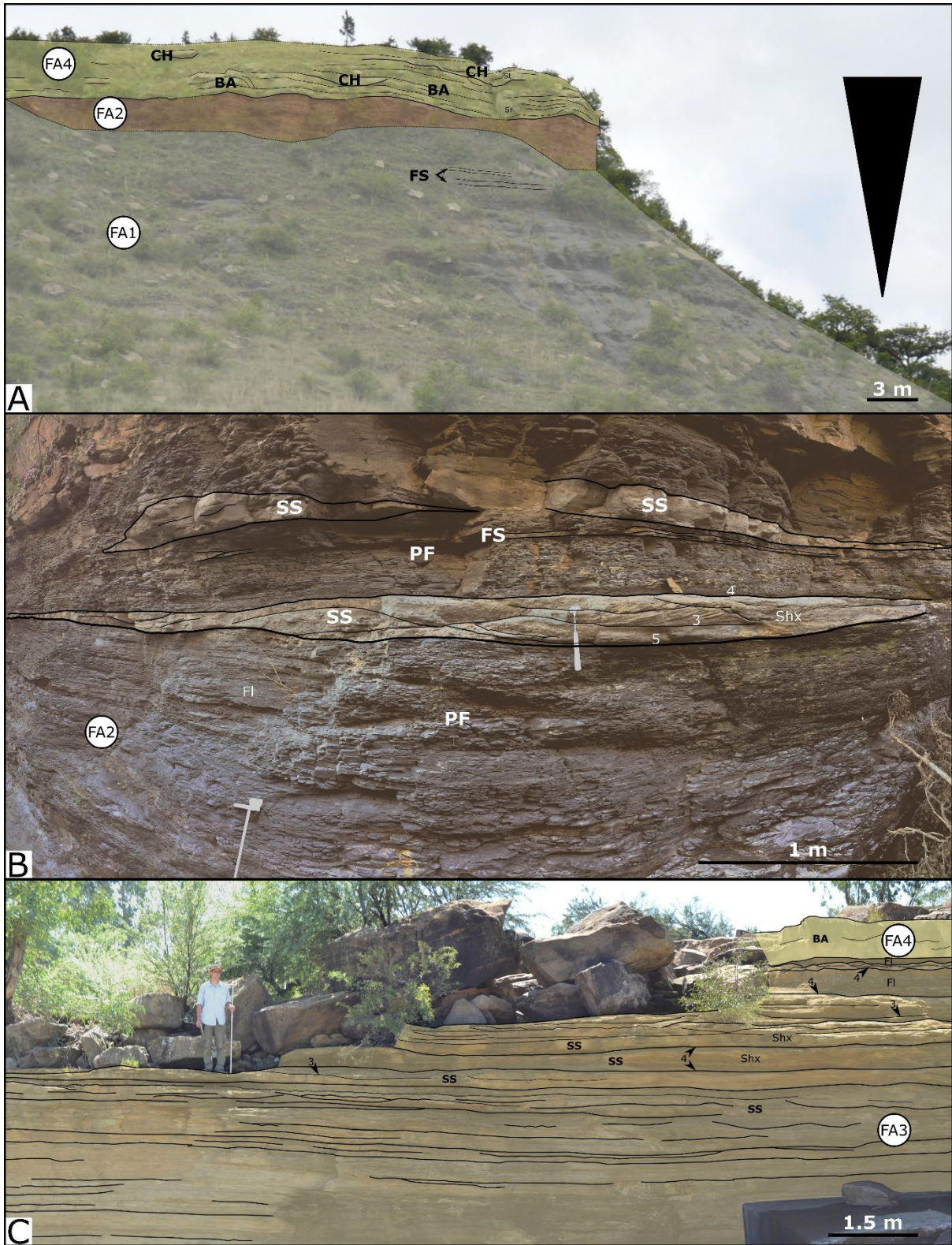


Figure 4 A) Field photograph and interpretive sketch overlay showing the overall upward coarsening trend of FA1, FA2, and FA4, and examples of Prodelta Fines (PF) and Frontal Splay (FS) architectural elements observed in FA1, FA2, and FA4, and Bar Accretion (BA) and Channel Fill (CH) architectural elements from FA4, at the locality Goewermentskop near Newcastle. B) Field photographs with interpretive sketch overlays showing examples of architectural elements Prodelta Fines (PF), Frontal Splay (FS), and Storm Sheets (SS) within FA2 on the farm Van der Merwe’s Kraal. C) Panel section with interpretive sketch overlay showing FA3 and FA4, characterised by lithofacies type Shx and Storm Sheet (SS) elements, sharply overlain by Bar Accretion (BA) elements from FA4 at the outflow of the Barend Wessel Dam, Kroonstad. Numbered arrows indicate order of bounding surfaces.



Figure 5 Examples of ichnofossils from Facies Association 1, Facies Association 2, and Facies Association 3 in the study area. Borehole cores: I and J = GR1/76; N = J82/6. Abbreviations for ichnogenera: Ar = *Arenicolites*; Co = *Cochlichmus*; Cr = *Cruziana*; Di = *Diplocraterion*; Gy = *Gyrochorte*; Lo = *Lockeia*; Op = *Ophiomorpha*; Pa = *Palaeophycus*; Pl = *Planolites*; Ro = *Rosselia*; Ru = *Rusophycus*; Sk = *Skolithos*; Te = *Teichichmus*; Th = *Thalassinoides*.

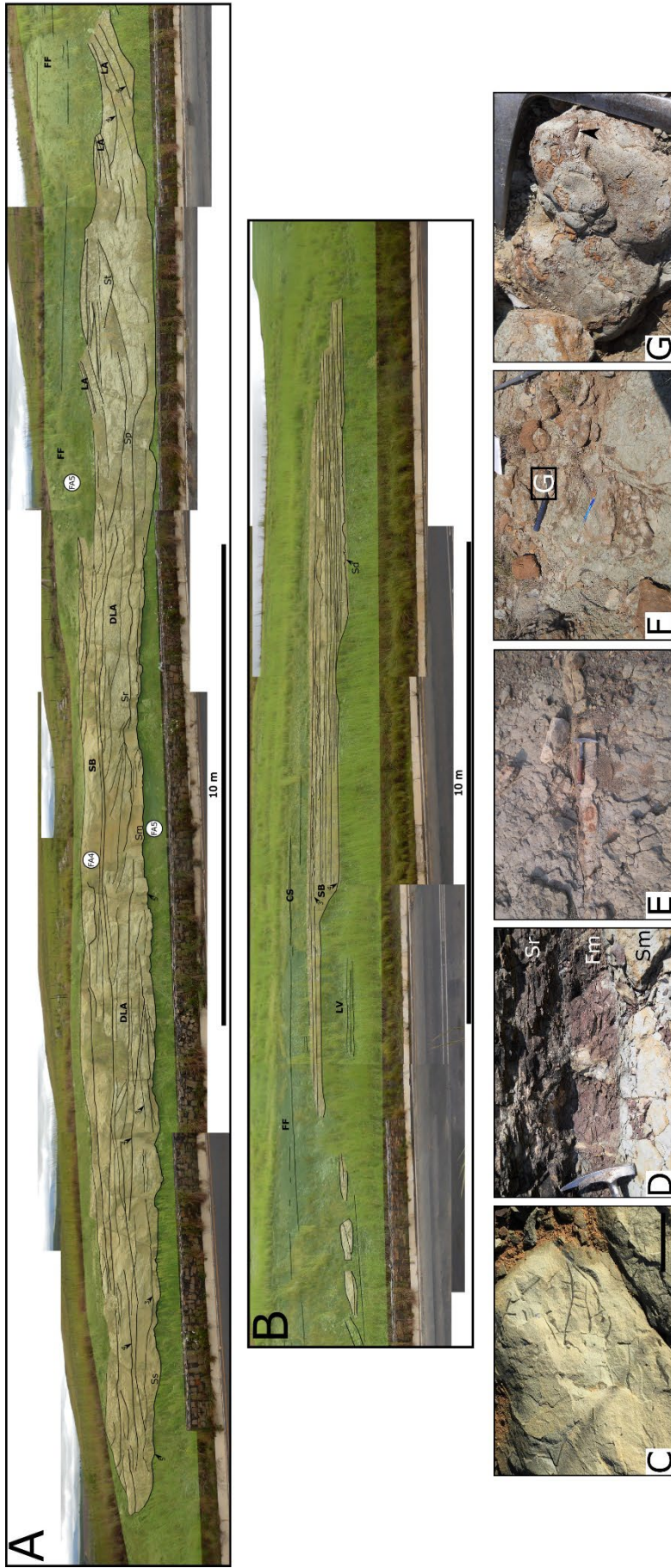


Figure 6 A and B) Panel section with interpretive sketch showing architectural elements (**bold**) and lithofacies (normal) characteristic of FA4 and FA5 at Rooinek Pass in the north-eastern Free State Province. Numbers indicate bounding surface order. C- G) Examples of sedimentological features observed in Facies Association 5, including C) Root traces in a siltstone of Facies Fm; D) sand-filled mudcracks, E) sandstone dykes, F and G) extensive nodular horizon with skull of the dicynodont *Diictodon* (tusk is arrowed).

1421
1422

Table 1 Descriptions and interpretations of lithofacies types (modified after Miall (2006); * denotes newly erected lithofacies types) from the studied stratigraphic interval in the northern part of the main Karoo Basin.

Lithofacies Code	Lithofacies	Description	Interpretation
Gmm	Matrix supported gravel	Matrix supported conglomerate with quartzite extraclasts up to 15 cm across. Poorly sorted, ungraded and may display crude bedding	Debris flow
Ss	Scour-fill sand	Medium to very coarse-grained sandstone with granule- to pebble-sized intraclasts and extraclasts. Common at base of channels	Lag deposit formed as scour-structures fill up during the waning phase of a flood
St	Trough cross-stratified sandstone	Medium- to coarse-grained sandstones with cross-stratification in which the lower bounding surfaces are curved and truncate other facies or cosets	Migration of three-dimensional dunes
Sh	Horizontally stratified sandstone	Well sorted, horizontally laminated and bedded. Occurs in fine- to medium-grained sandstones	Plane-bed flow (upper flow regime)
Sp	Planar cross-bedded sandstone	Fine- to coarse-grained sandstones in which the foresets dip between 15° and 35°	Migration of two-dimensional dunes
Sr	Ripple cross-laminated sandstones	Very fine- to medium-grained sandstones with ripple cross-laminations	Lower flow regime, wave and wind induced ripples
Sm	Massive or weakly graded sandstone	Very fine- to coarse-grained sandstones in which no internal sedimentary structures are observed	Rapid deposition e.g. sediment gravity flows. Alternatively, loss of sedimentary structures could be due to bioturbation and/ or weathering
Sa*	Sandstone with floating mudstone clasts	Fine- to medium-grained sandstones containing thin argillaceous acicular structures throughout. Ripple cross-lamination and horizontal bedding may be present	Rapid subaqueous deposition by turbidity currents
Sd*	Sandstone/siltstone beds with deformation structures	Fine-grained sandstone and siltstone beds that display soft-sediment deformation structures including load casts, ball and pillows, and water escape and flame structures	Rapid sedimentation, liquefaction, reverse density gradation, shear stress, or collapse of channel banks
Shx*	Hummocky cross-stratified sandstone	Medium-grained sandy units displaying large wave-form internal laminae, comprising almost flat-to-low angle negative relief convex-down swales and positive relief convex-up hummocks	Deposition on the shoreface and shelf environments under the influence of both oscillatory and unidirectional currents related to storm activity
R*	Rhythmically interbedded mudstones, siltstones, and sandstones	Alternating heterolithic beds of fine- to medium-, and occasionally coarse-grained sandstones, siltstones, and mudstones. Lower bounding surface of coarser beds is sharp, whereas the upper bounding surface commonly has symmetrical ripple marks	Deposition in parts of the interdistributary bay proximal to subaqueous distributary channels. Finer-grained argillaceous beds were deposited through suspension settling during periods of lower energy while the interbedded coarser-grained beds were deposited under higher energy conditions

Fl	Laminated siltstones and mudstones	Relatively thick (> 0.5 m) successions of horizontally and ripple-cross laminated mudstones	Suspension settling, or deposition under lower flow regime conditions. Depositional settings include distal interdistributary bays, lagoons, and on tidal flats; away from channels and where wave activity is minimal. Fluvial settings include ephemeral floodplain pools and ponds
Fm	Massive siltstones and mudstones	Massive beds of siltstone and mudstone displaying no apparent bedding planes. Co-occurs with Facies Fl and thin sandstone lenses may be present	Either through suspension settling, with bioturbation, diagenesis, or weathering resulting in the lack of sedimentary structures, or through rapid deposition e.g. hyperpycnal/hypopycnal flows
C	Carbonaceous black shales and coal	Finely to very finely laminated, highly carbonaceous shales containing thin beds and lenses of coal up to 0.5 m thick	Suspension settling of fines in low-lying interchannel plains, abandoned channels and backswamp environments on the upper delta plain and flood plain. Peat deposits or other accumulations of organic matter gave rise to thin coal seams
Ca	Carbonate horizon	Laterally extensive (10 – 30 m) carbonate horizons, commonly 30 – 50 cm thick. Upper and lower bounding surfaces are either straight or irregular, with sharp contacts	Deposition under waterlogged or palustrine conditions on the floodplain

1423

1424
1425
1426
1427

Table 2 Description and interpretation of the architectural elements from the studied stratigraphic interval in the northern part of the main Karoo Basin. Modified after Miall (1985), Miall (2006), Colombero et al. (2013), Platt and Keller (1992), Gani and Bhattacharya (2007), and Ahmed et al. (2014). See Table 1 for descriptions of lithofacies types.

Architectural element Code	Architectural element	Description	Interpretation
PF	Prodelta Fines	Aerially extensive fine-grained body with sheetlike geometry and bounded by third-order surfaces. Comprised of laminated to massive mudstones, siltstones (lithofacies types Fl and Fm), and subordinate very fine- to fine-grained lenticular sandstones	Deposition in very low-to-low energy conditions, mainly through suspension settling (Fl) or by hypo- and hyperpycnal flow processes (Fm)
FS	Frontal Splay	5 to 50-cm-thick sandstones bound by third- to fourth-order surfaces. Consists of sandstone beds, with sharp, sometimes erosional bases, and that are often continuous across the outcrop. Internally, sandstone beds may be structureless, horizontally-, and/or ripple cross-laminated	Non-channelized sediment gravity flows, potentially originating from high sediment discharge during river floods, slump failures at a river mouth, and/or storm resuspension of bottom sediments
SS	Storm Sheet	Hummocky-cross stratified sandstones bounded by third- or fourth-order surfaces. Can comprise either single or stacked beds of lithofacies type Shx	Deposition and reworking of sediment on the lower to middle delta front or shoreface by storms and waves
CH	Channel Fill	Sandstones bound by third- to fifth-order surfaces. CH elements have a concave-up, often erosive base, whereas the upper bounding surface can be sharp or gradational. Multi-storey fills are common, with each storey bounded by an erosional surface and smaller channels that overlap and crosscut one another	Aggradational channel fill in active channels
BA	Bar Accretion	Flat to sloping, lens shaped sandstones bounded by third- or fourth-order surfaces. Internal sedimentary structures include Sd, Sm, Sr, St, Sh, and occasionally Shx	Produced mainly by river-fed currents and sediments. Deposition via migration of dunes. Increase or decrease in the flow velocity is recorded by lithofacies types Sh and Sr, respectively. Occasional Shx indicates periodic storm reworking of the bars, while the lithofacies types Sm and Sd suggest rapid deposition and dewatering of sediments

SG	Sediment-Gravity-Flow Deposits	Narrow, elongate lobes or multistorey sheets that may be intimately interbedded with element SB. Can have a channelised form. Boundaries are irregular, often nonerosive, and beds may have an irregular shape. Internally a wide variety of textures and fabrics may be present, although a chaotic fabric is common. Lithofacies types include Gmm, Sa, Sd, and Sm	Debris flows with high sediment concentration. The flows often occupy existing erosion channels, or the irregular topography formed by a previous flow or sheet flood event, thereby taking on a channelised form
SB	Sandy Bedforms	Tabular sheets or lenticular sandbodies that have flat, sometimes slightly erosive, bases and sharp upper surfaces. Element SB occurs as isolated or stacked tabular sand bodies and is commonly infilled with lithofacies types Sh, Sp, St, and Sr. Internal bounding surfaces are of the first- to third-order	This element forms under conditions where trains or fields of individual bedforms accumulate predominantly through vertical aggradation as opposed to lateral or downstream accretion (LA or DA elements). SB elements can form within channels, as channel floor dune fields or shallow channel fill and bar top assemblages, or as a result of unconfined flows during flood events. Changes in flow regime, either long- or short-term, results in the vertical stacking of different bedform types
LA	Lateral Accretion	Slightly concave upward sandstone bodies, often with erosional bases, and containing dipping third-order internal bounding surfaces	Lateral accretion of sediment (oblique to the palaeo-flow) within a channel, as opposed to the vertical aggradation of sandy bedform (SB) and channel elements (CH), or downstream accretion (DA)
DA	Downstream Accretion	Sandstone bodies with internal bounding surfaces that dip gently (<10°) in a downstream direction and enclose cosets of downstream orientated flow-regime bed-forms with second- and third-order internal erosion surfaces, and 4th order bounding surfaces. DA elements typically have a flat or channelled base and convex-up profile. Where palaeocurrent direction cannot be determined, LA/DA is used	Accretion of sediment in the downstream direction
DLA	Downstream and Lateral Accretion	Sandstone bodies that typically have a wedge or lens geometry. Intermediate bar forms between DA and LA elements. Bedding geometries demonstrate dominantly oblique accretion due to downstream accretion on the downstream end and cross-bar accretion along the flank	Formed when downstream and lateral accretion occurs in comparable proportions
FF	Overbank (floodplain) Fines	Tabular to prismatic bodies of fine-grained deposits (lithofacies types Fm and Fl) bounded by planar surfaces. Laterally persistent depositional increments tend to be vertically stacked and pedogenic alteration is common	Aggradational deposits from suspension setting on the floodplain

AC	Abandoned Channel	Heterolithic bodies with a similar geometry to Channel Fill (CH) elements. Dominated by vertically stacked facies. Lithofacies types F1 and Fm are predominant	Deposition in lower energy conditions e.g. in ponded waters of an abandoned reach, where suspension settling is predominant and stream flow processes are intermittent
CS	Crevasse Splay	Tongue- or lobe-shaped sandstone bodies bordering the channel margins and bounded by fourth-order surfaces. CS elements have flat, sharp, and sometimes erosive bases, and often thin away from the channel margins, interfingering or grading laterally into other elements, mainly FF	Periodic unconfined flow emerging from a channel onto the floodplain
LV	Levées	Rhythmically bedded mudstone/siltstone and ripple-laminated sandstone. Has the form of tapering wedges that thin and fine away from channel-belt margins. Fine-scale loading, water escape and slump structures (lithofacies type Sd) may be present. Base is often poorly defined and internal accretion surfaces offlap and/or downlap at low angles (2° – 10°). Palaeo-flow direction is usually oriented at high angles to the channel border	The most proximal overbank deposits. Deposited in areas separating the channel from the floodplain. Loading and water escape structures indicate high sedimentation rates

1428

1429
1430

Table 3 Characteristics of the five facies associations encountered in the studied stratigraphic interval in the northern part of the main Karoo Basin.

Facies Association	Lithofacies present	Architectural elements	Ichnogenera
Facies Association 1: Prodelta	Fl; Fm	PF; FS	<i>Thalassinoides</i> , <i>Planolites</i> , limulid trackways
Facies Association 2: Delta front	Sh; Sr; Sm; Sd; Shx; R; Fl; Fm	FS; SS	<i>Arenicolites</i> , <i>Cochlichnus</i> , <i>Diplocraterion</i> , <i>Lockeia</i> , <i>Gyrochorte</i> , <i>Gordia</i> , <i>Ophiomorpha</i> , <i>Palaeophycus</i> , <i>Planolites</i> , <i>Rosselia</i> , <i>Rusophycus</i> , <i>Skolithos</i> , <i>Teichichnus</i> , and <i>Thalassinoides</i>
Facies Association 3: Lower shoreface	Shx; R; Fl; Fm	SS	<i>Arenicolites</i> , <i>Cruziana</i> , <i>Gyrochorte</i> , <i>Ophiomorpha</i> , <i>Palaeophycus</i> , <i>Planolites</i> , <i>Rosselia</i> , <i>Skolithos</i> , and <i>Thalassinoides</i>
Facies Association 4: Confined channelised system	Gmm; Ss; Sm; Sh; St; Sr; Sp; Sa; Sd	CH; BA; SG; SB; LA; DA; DLA	
Facies Association 5: Floodplain fines and overbank deposits	Ss; Sh; Sr; Sm; Sd; Fl; Fm; C; Ca	FF; AC; CS; LV	

1431

Table 4 Representative taxonomic list of tetrapod fossils that have been recovered from the study area.

Formation	Biozone	Clade	Species
Balfour Formation	<i>Cistecephalus</i> -to- <i>Daptocephalus</i> Assemblage Zone	Anomodontia	<i>Diictodon feliceps</i>
			<i>Pristerodon mackayi</i>
			<i>Endothiodon bathystoma</i>
			<i>Compsodon Helmoedi</i>
			<i>Dicynodontoides recurvidens</i>
			<i>Cistecephalus microrhinus</i>
			<i>Oudenodon bainii</i>
			<i>Aulacephalodon baini</i>
			<i>Kitchinganomodon crassus</i>
			<i>Rhachiocephalus magnus</i>
			<i>Dicynodon lacerticeps</i>
			<i>Daptocephalus leoniceps</i>
			<i>Dinanomodon gilli</i>
			<i>Basilodon woodwardi</i>
			<i>Lystrosaurus maccaigi</i>
		<i>Lystrosaurus curvatus</i>	
		Therocephalia	<i>Zorillodontops gracilis</i>
			<i>Moschorhinus kitchingi</i>
			<i>Theriognathus microps</i>
		Biarmosuchia	Burnetiidae indet.
Cynodontia	Cynodontia indet.		
Gorgonopsia	Gorgonopsia indet.		
Amphibia	<i>Uranocentrodon senekalensis</i>		
	<i>Laccosaurus watsoni</i>		
Abrahamskraal Fm.	<i>Tapinocephalus</i> Assemblage Zone	Anomodontia	<i>Robertia broomiana</i>
			<i>Eosimops newtoni</i>
			<i>Pristerodon mackayi</i>
		Therocephalia	<i>Glanosuchus macrops</i>
			<i>Pristerognathus polyodon</i>
		Pantestudines	<i>Eunotosaurus africanus</i>
		Amphibia	Rhinesuchidae indet.